Experimental Spectroscopy for Fusion Applications

M. Goto
National Institute for Fusion Science, Japan

colors and plasma constituents

- plasmas show different colors with different working gas
- guessing constituents of the plasma is a kind of plasma spectroscopy
- however, color is unsuitable for quantitative analysis

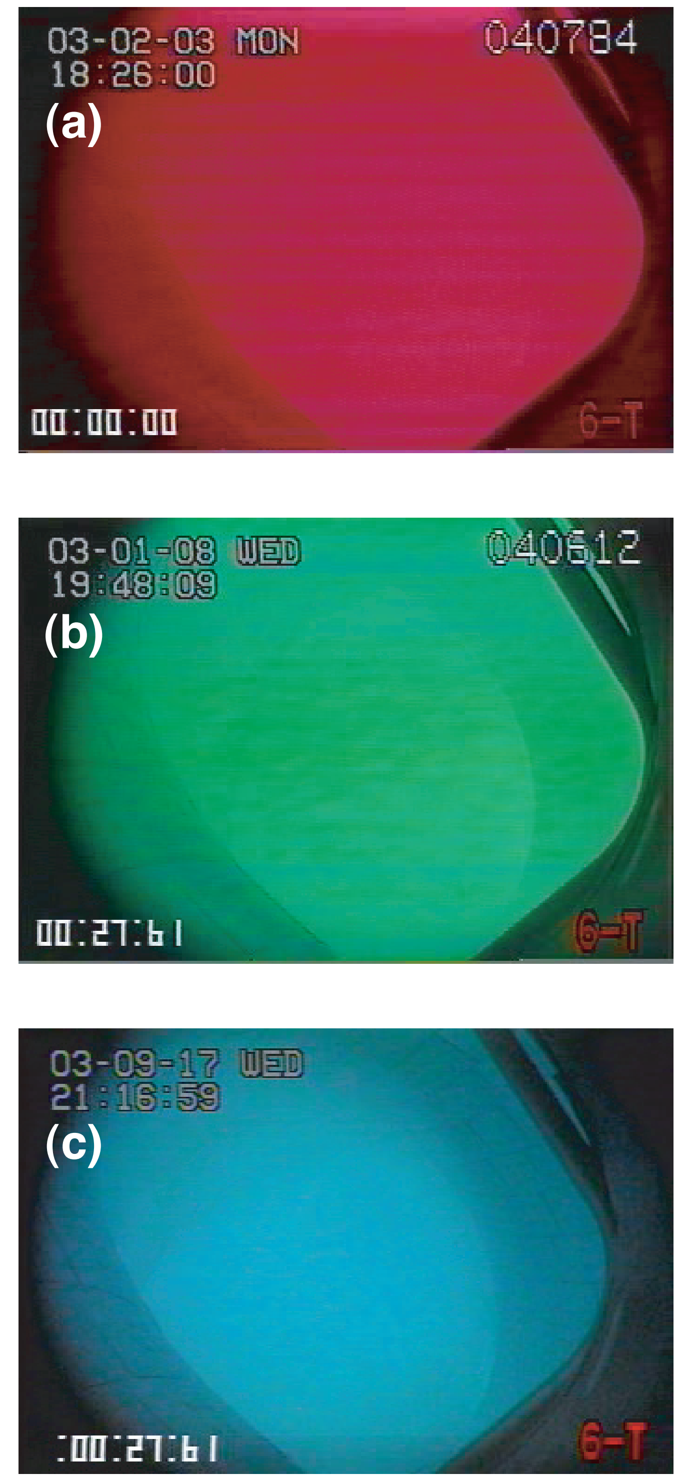

spectral measurement

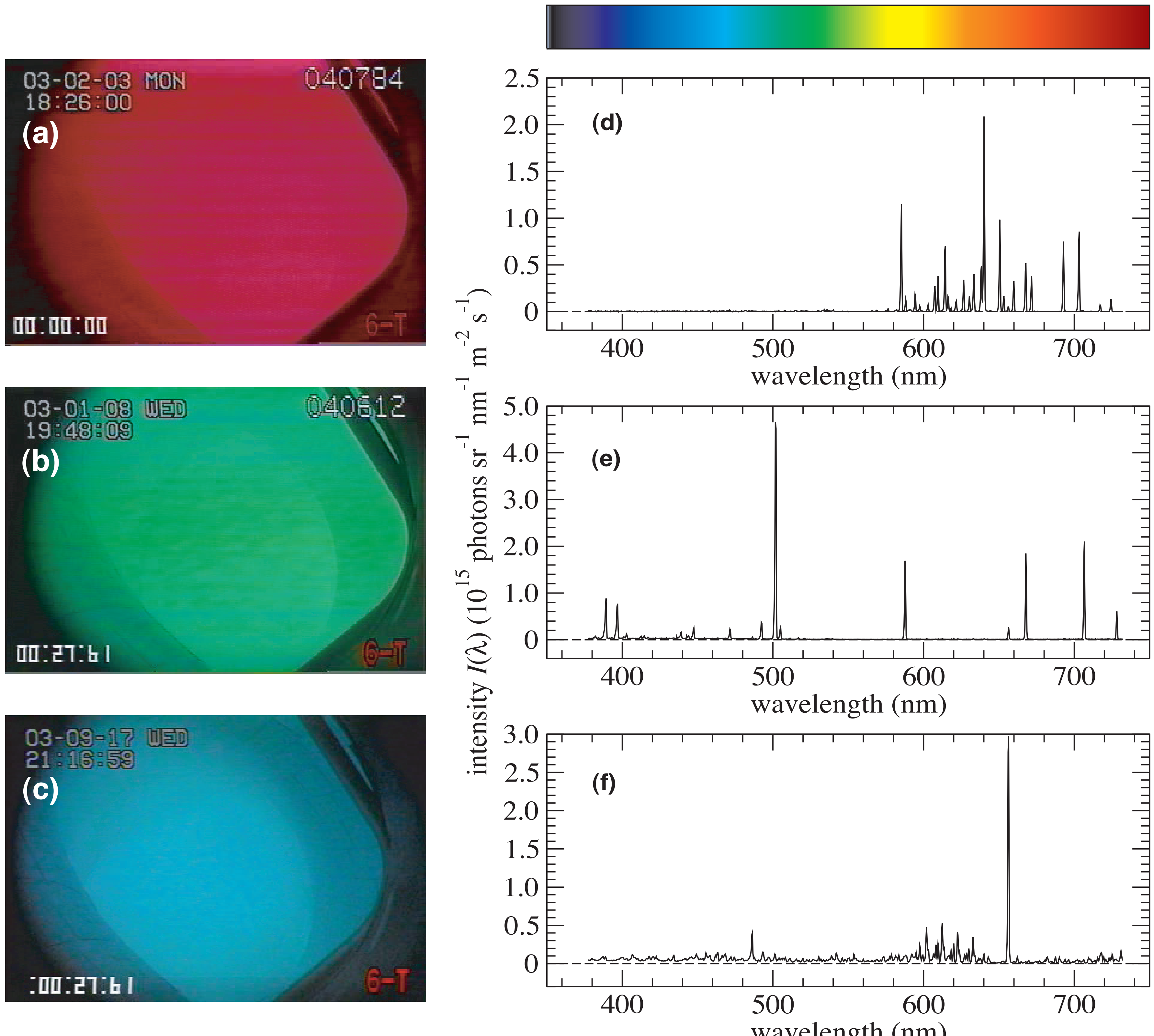

radiance and irradiance

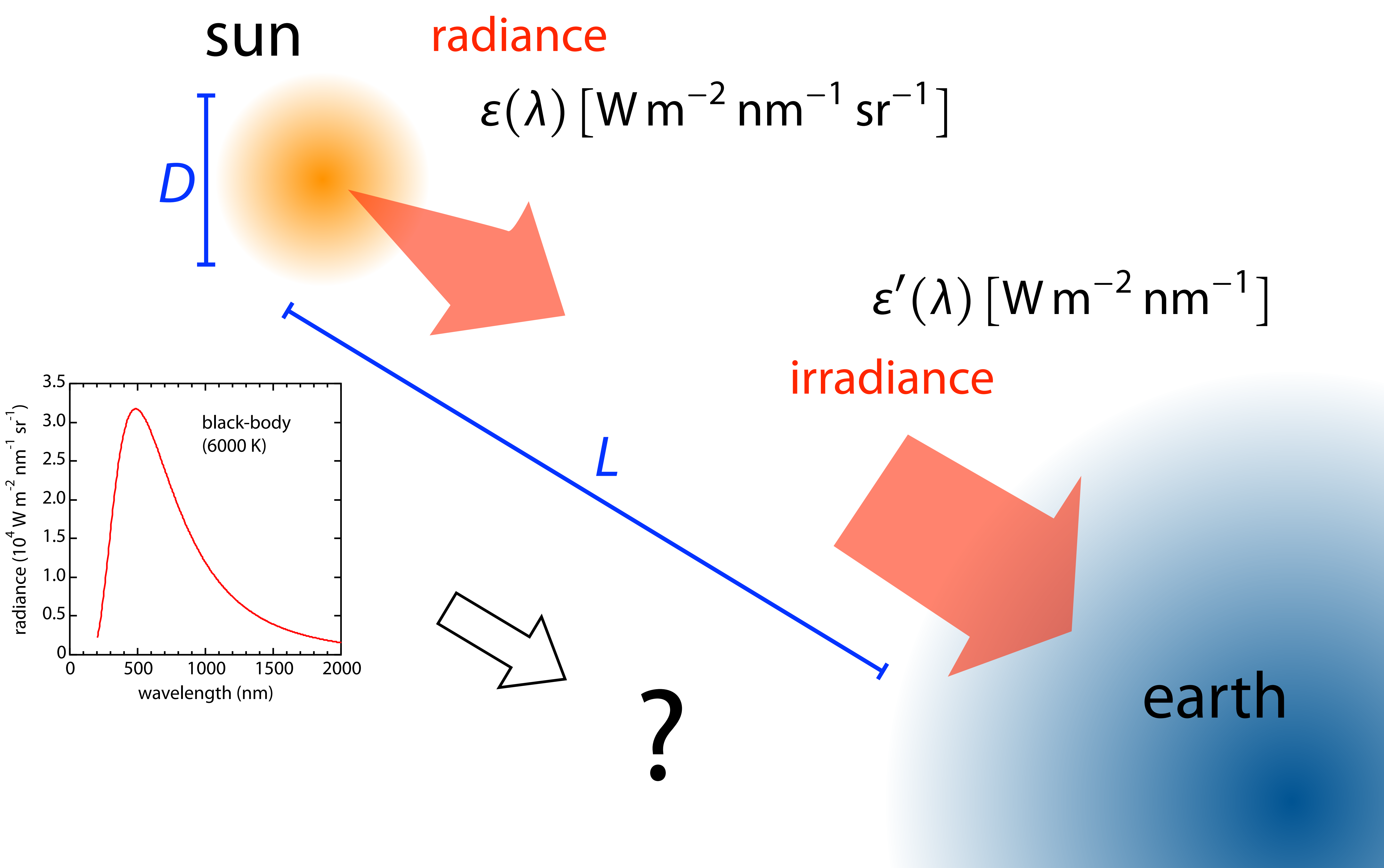

- mean distance from earth

$$L = 1.496 \text{ x } 10^{11} \text{ m}$$

- mean diameter

$$D = 1.392 \text{ x } 10^{9} \text{ m}$$

$$\varepsilon'(\lambda) = \varepsilon(\lambda) \times \pi \left(\frac{D}{2}\right)^2 \times \frac{1}{L^2}$$

6.8×10^{-5}

apparent surface area of the sun

solid angle of 1m^2 area on earth

$\varepsilon(\lambda)$ → $\varepsilon'(\lambda)$

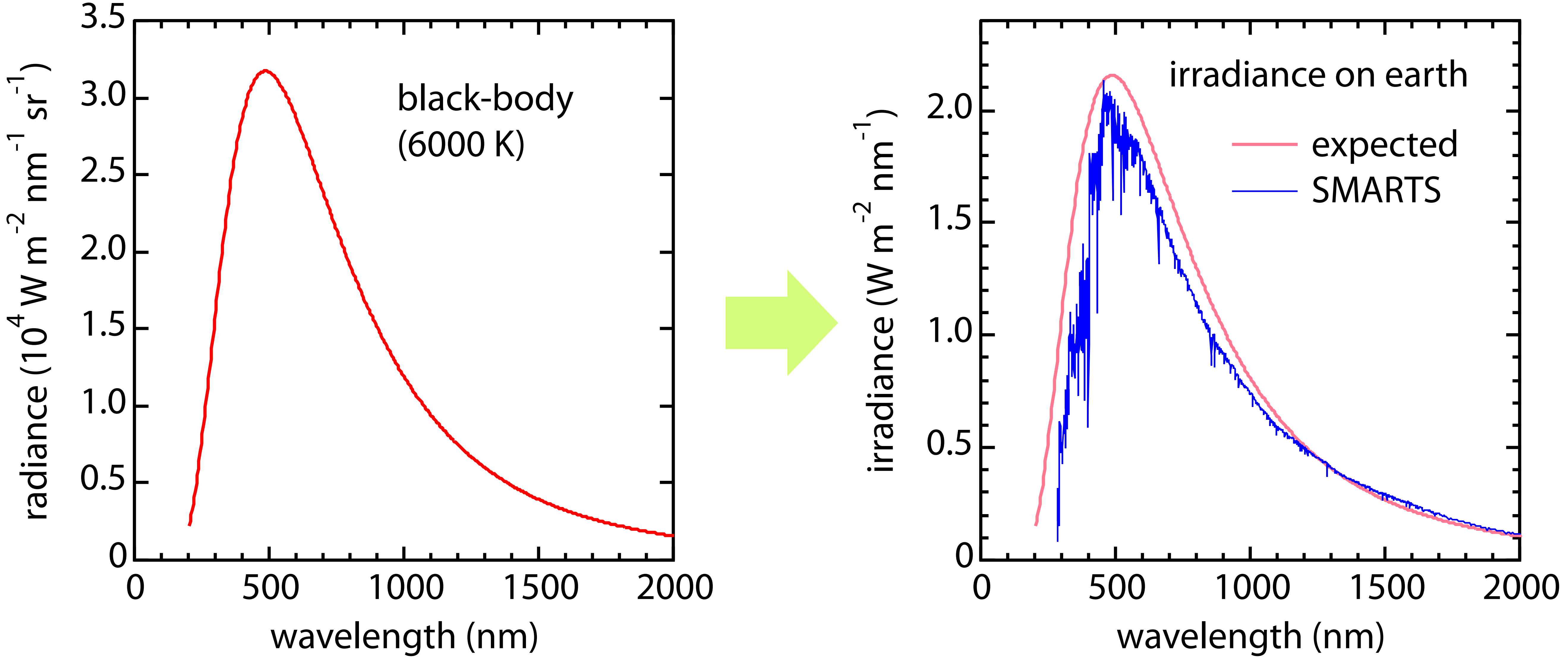

SMARTS (Simple Model of the Atmospheric Radiative Transfer of Sunshine)
http://www.nrel.gov/rredc/smarts/

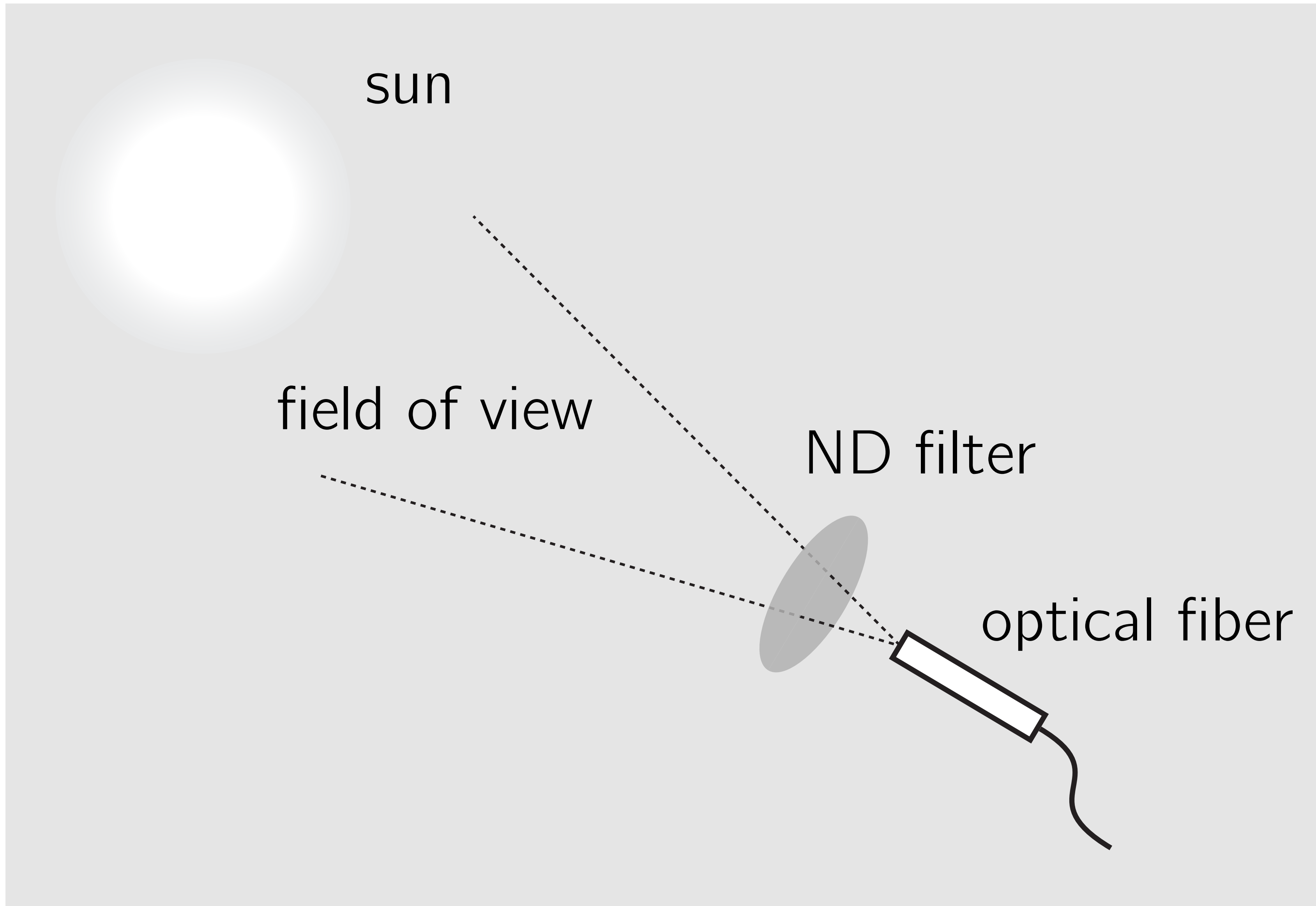

Figure 2: Arrangement for the direct observation of the solar radiation.

$$W'(\lambda) = \frac{\Gamma(\lambda)}{a} = \frac{s}{x^2} W(\lambda) \quad [\mathrm{W\,m^{-2}\,nm^{-1}}].$$

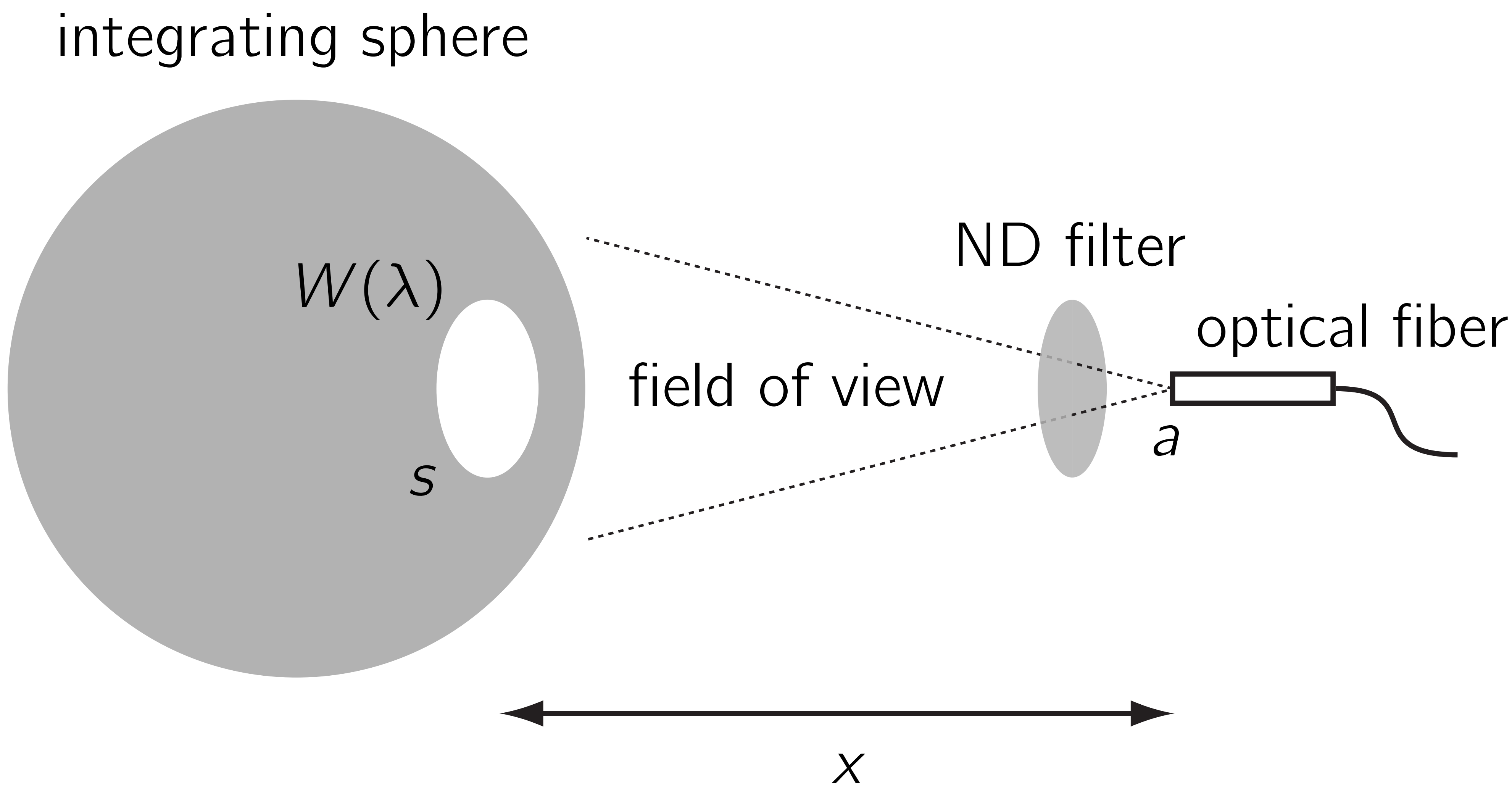

Figure 1: Optical arrangement for sensitivity calibration.

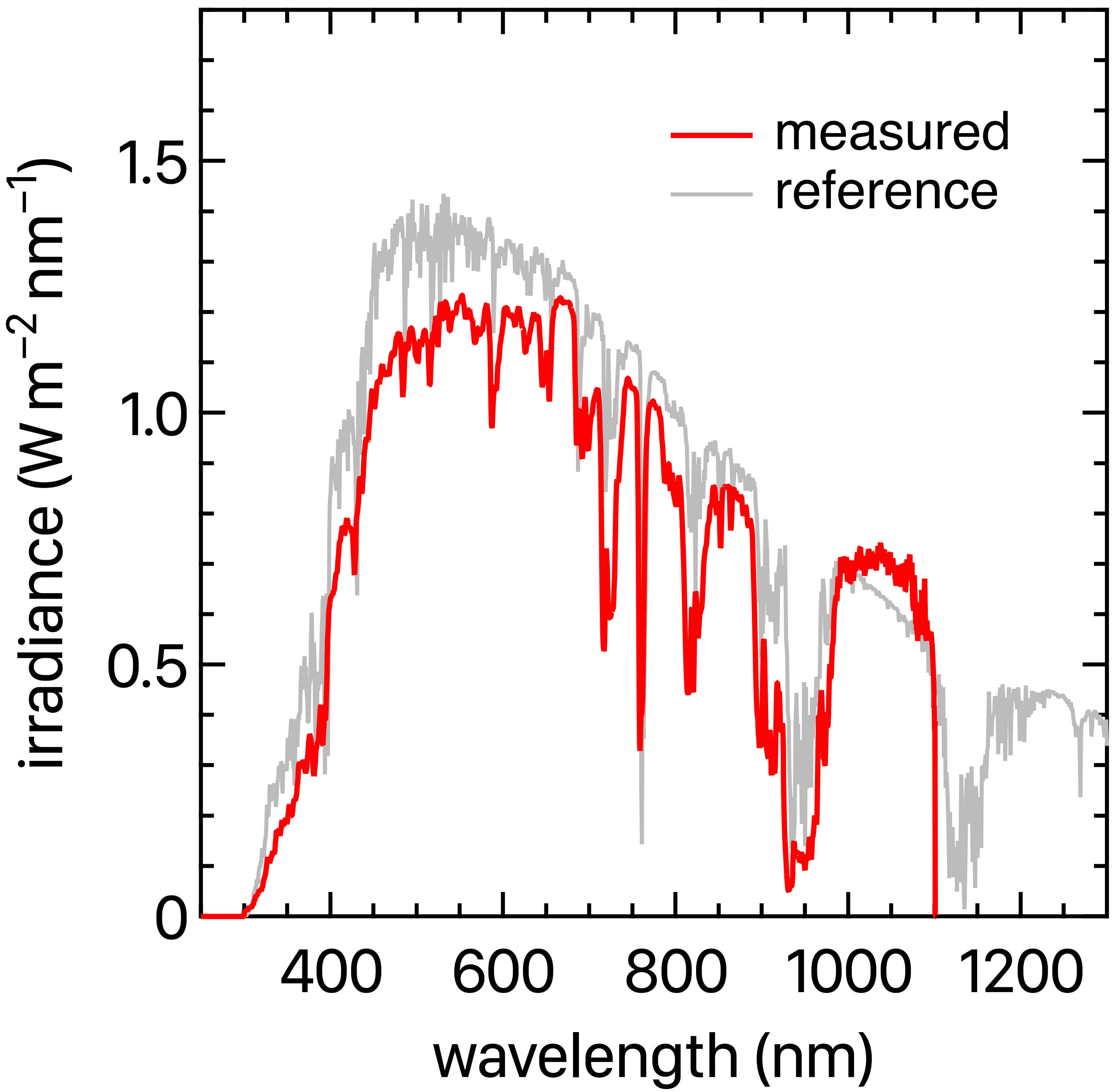

reference: www.astm.org/g0173-03r20.html

Large Helical Device (LHD)

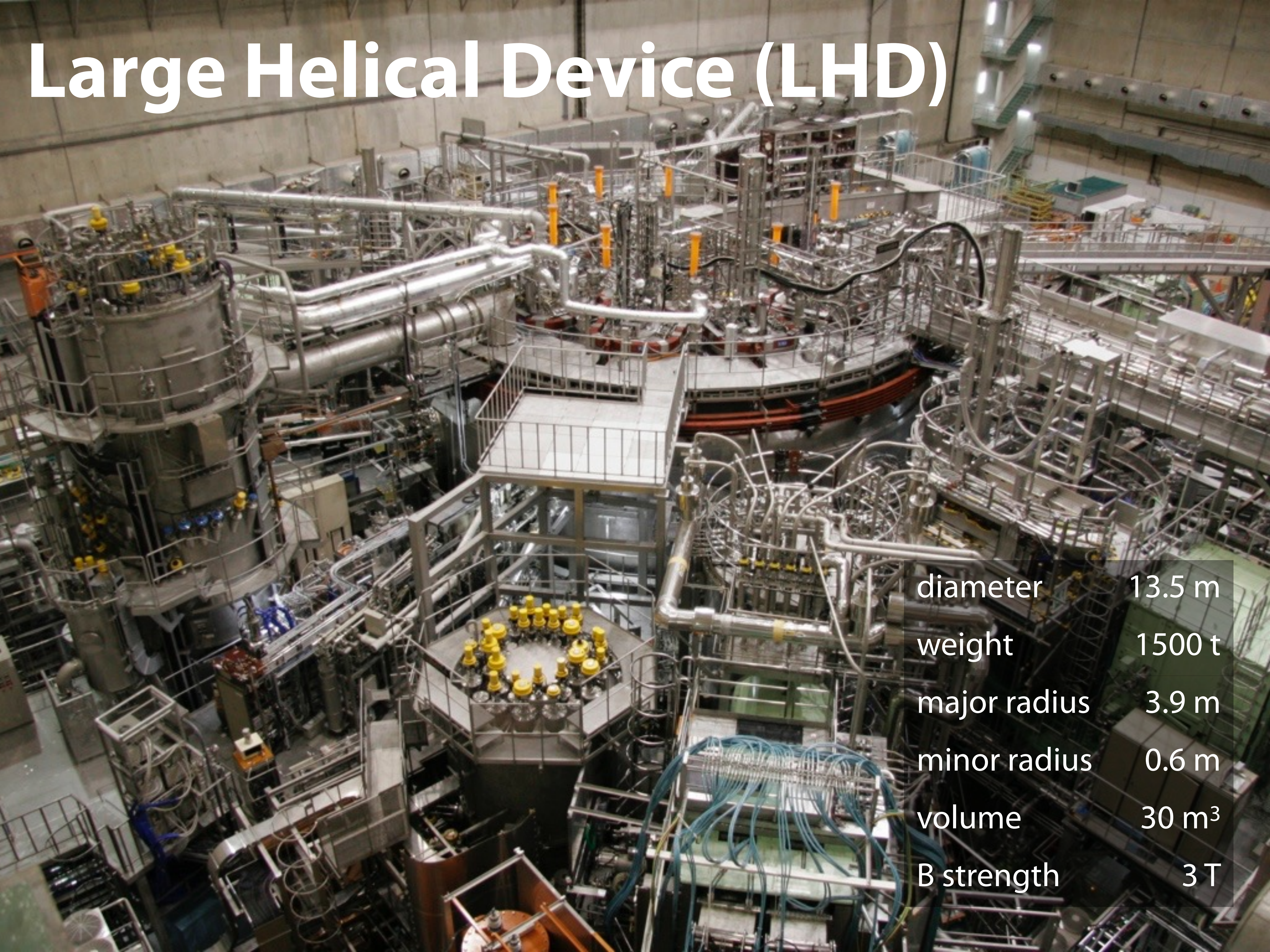

diameter	13.5 m
weight	1500 t
major radius	3.9 m
minor radius	0.6 m
volume	30 m^3
B strength	3 T

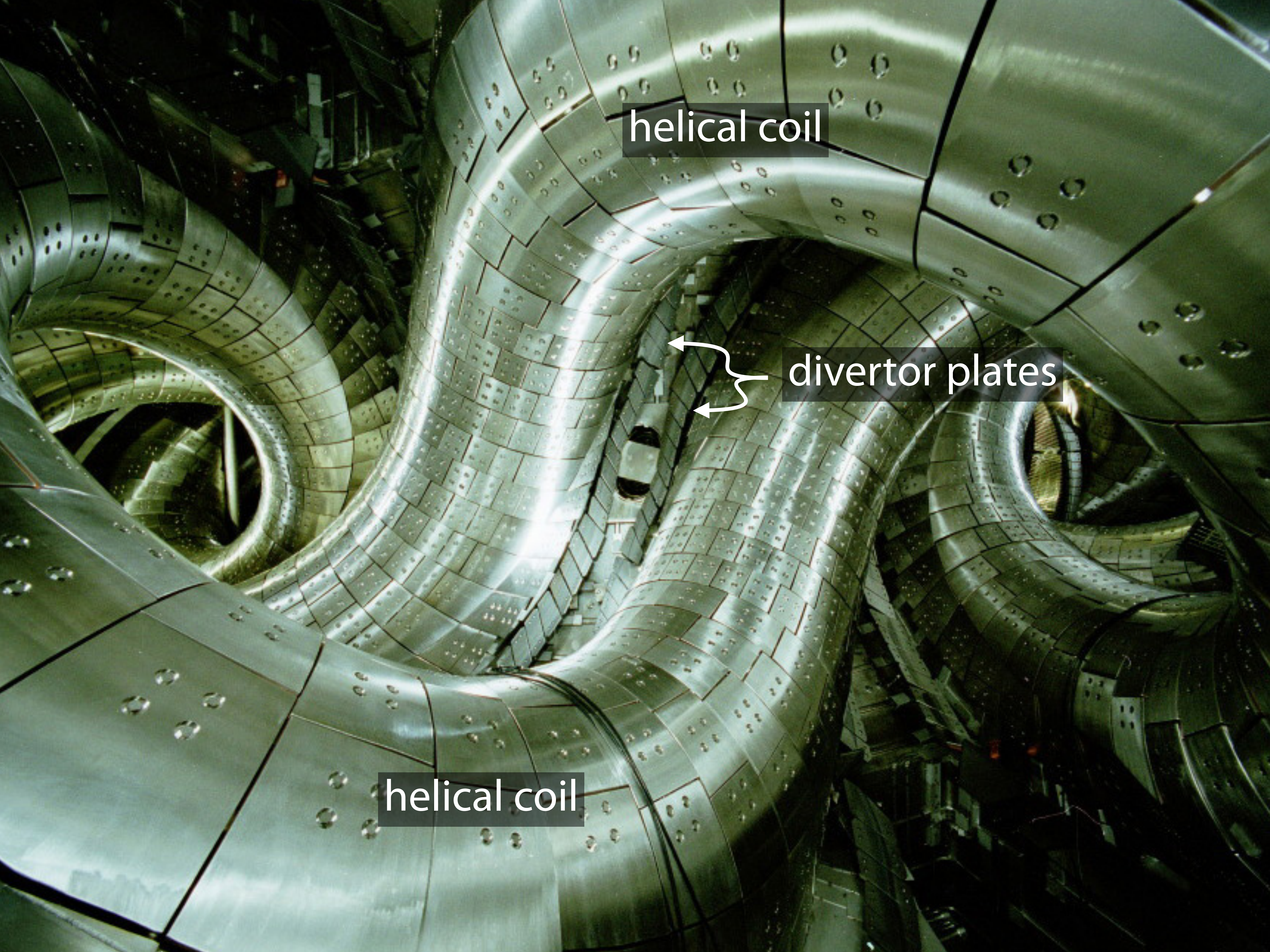
helical coil
divertor plates
helical coil

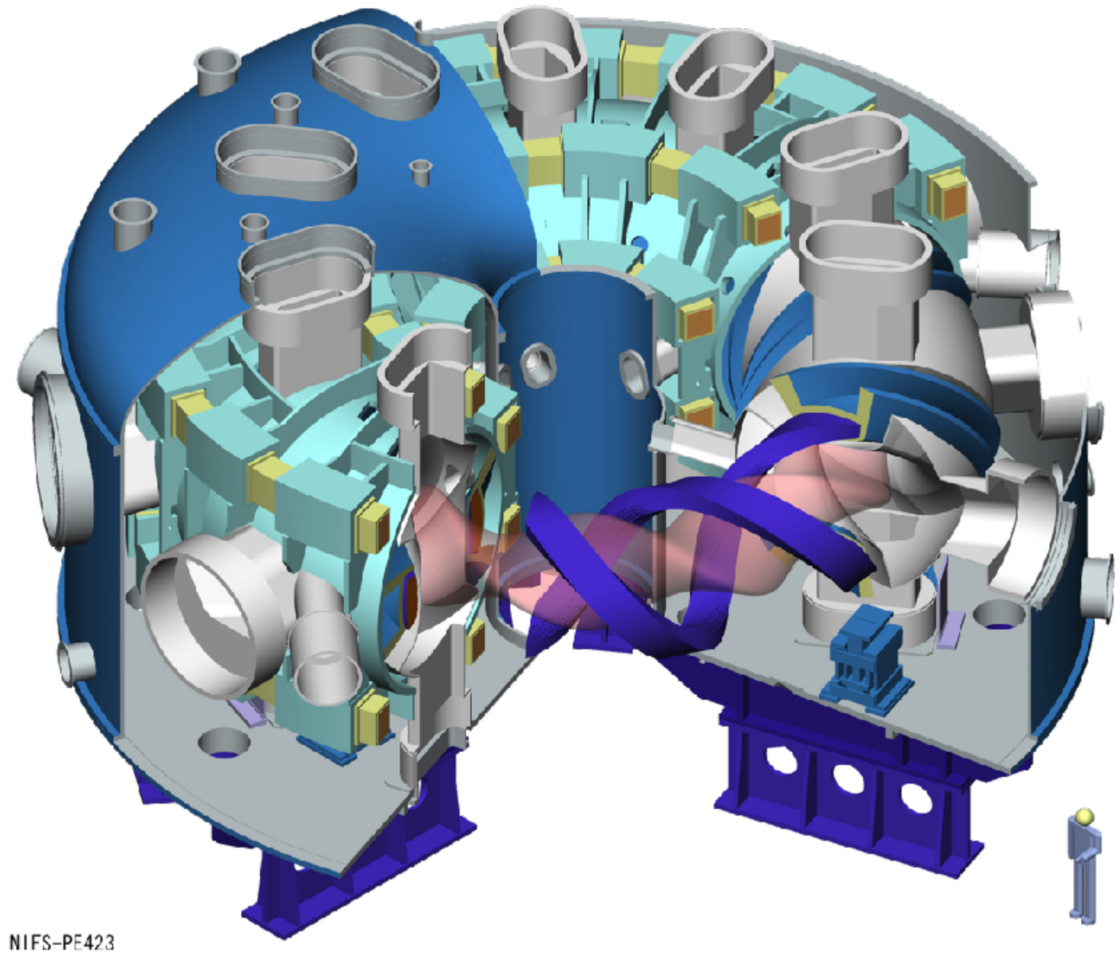

- heliotron-type device, i.e., no inductive plasma current
- advantageous for steady-state operation (no disruption)

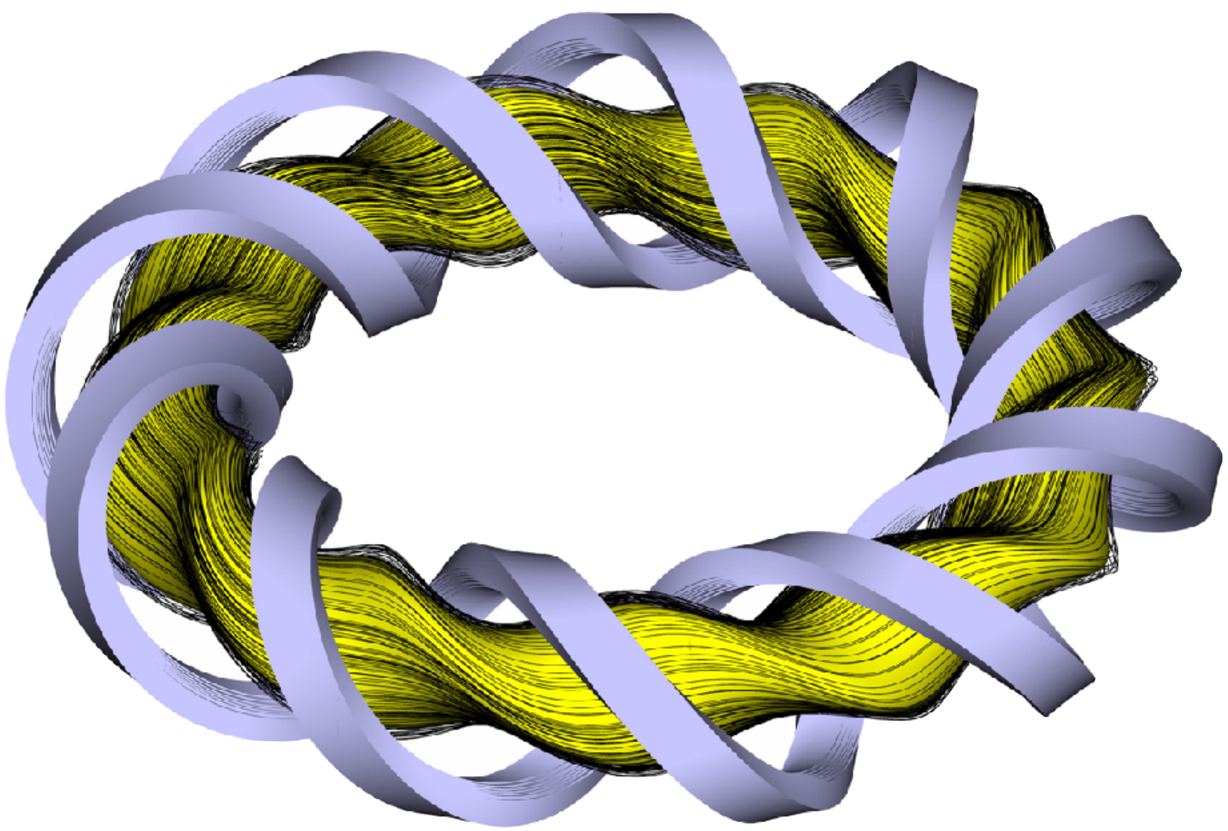

achievements

T_e	20 keV
T_i	10 keV
n_e	10^{21} m^{-3}

- spectroscopic diagnosis can be classified into two categories
- high wavelength resolution measurement
  - shift, broadening, splitting, etc.
- wide wavelength range measurement
  - intensity distribution of various emission lines, line intensity ratio, continuum

<table>
<tr><th colspan="2">observable</th><th>obtainable</th><th></th></tr>
<tr><td colspan="2">shift</td><td>ion velocity</td><td rowspan="5">high resolution measurement</td></tr>
<tr><td rowspan="2">splitting</td><td>Zeeman</td><td>magnetic field</td></tr>
<tr><td>Stark</td><td>electric field</td></tr>
<tr><td rowspan="2">broadening</td><td>Doppler</td><td>T_i</td></tr>
<tr><td>Stark</td><td>n_e</td></tr>
<tr><td colspan="2">intensity ratios
intensity distribution</td><td>T_e, n_e
ionizing or recombining</td><td rowspan="2">low resolution measurement</td></tr>
<tr><td colspan="2">intensity</td><td>n_i</td></tr>
</table>

line intensity distribution

- various emission lines are simultaneously measured
- population distribution over excited levels gives information on the plasma state
- collisional-radiative model is used for the analysis


116554
00:00:04:31
6-T

main discharge with helium gas

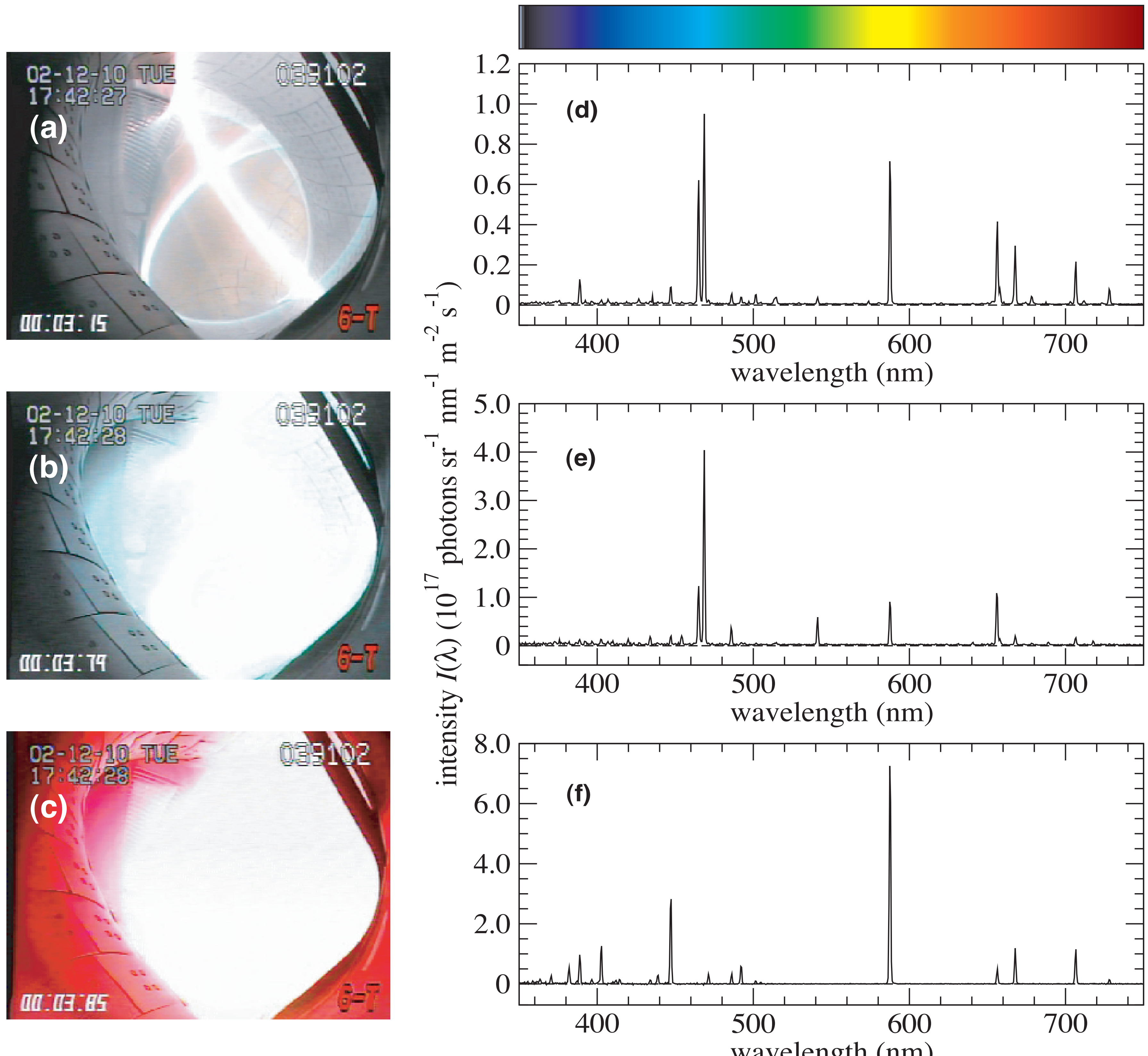

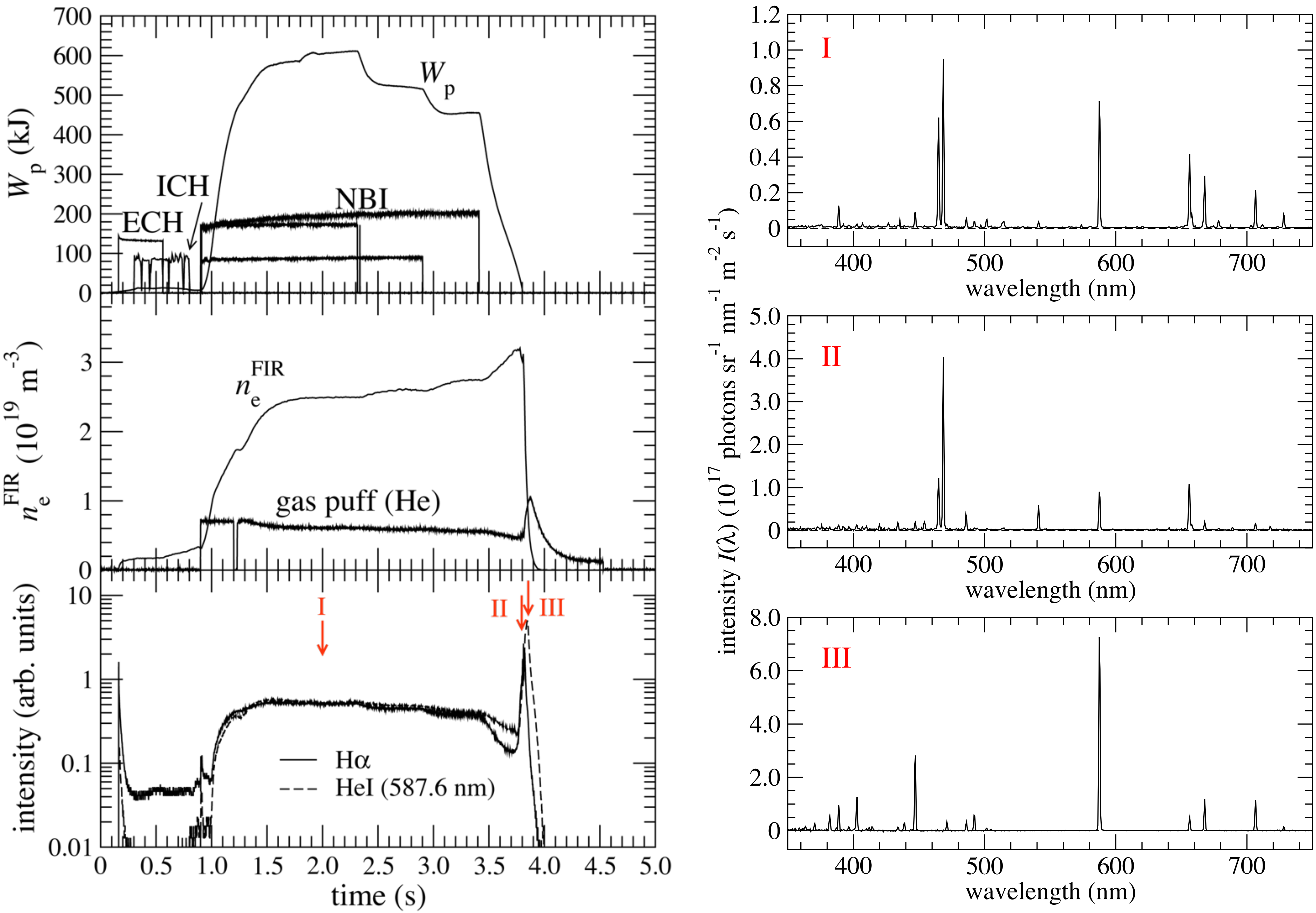

W_p
ICH
ECH
NBI
W_p (kJ)
n_e^FIR
gas puff (He)
n_e^FIR (10^19 m^-3)
I
II
III
Hα
HeI (587.6 nm)
intensity (arb. units)
time (s)
wavelength (nm)
intensity I(λ) (10^17 photons sr^-1 nm^-1 m^-2 s^-1)

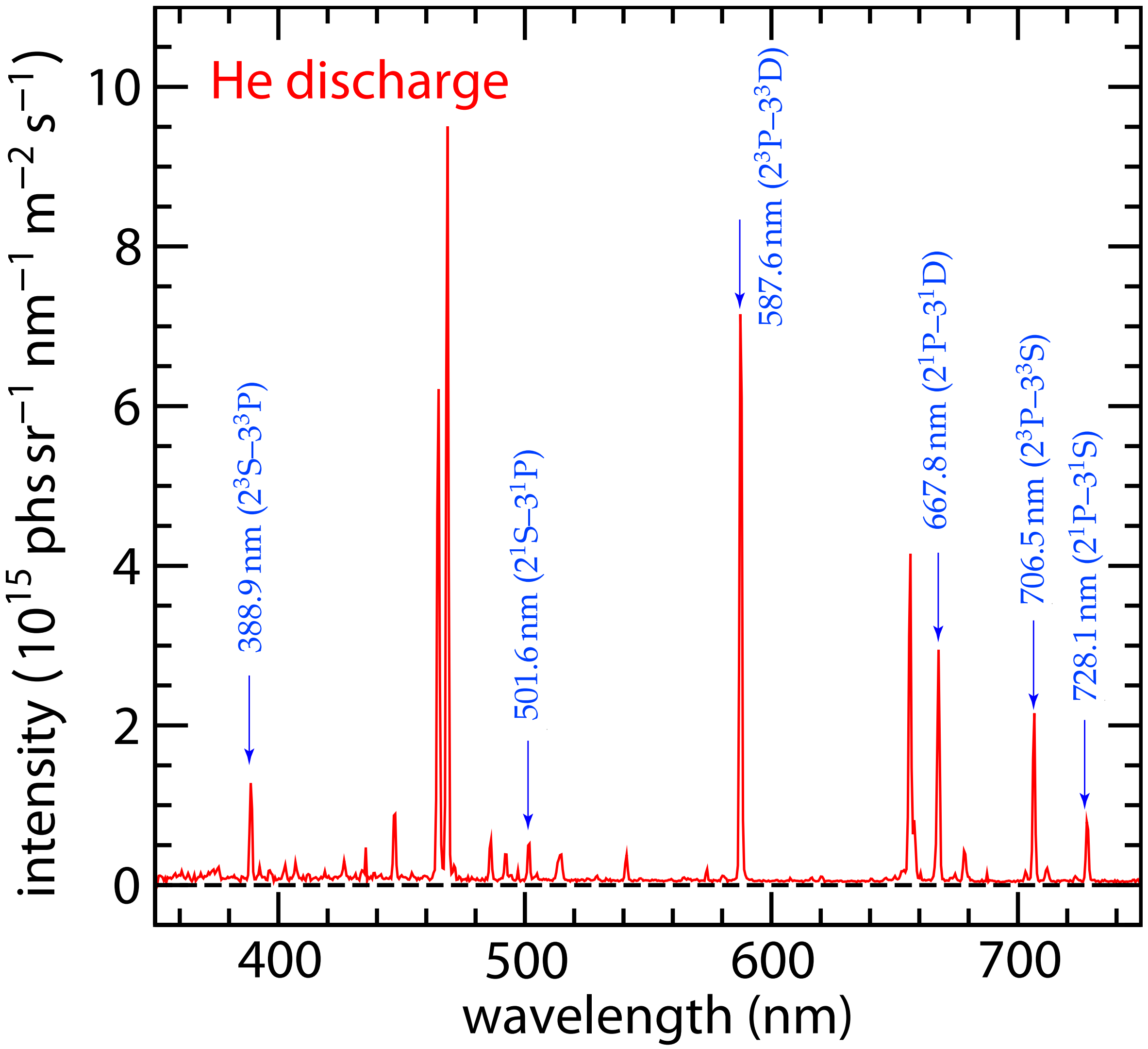
He discharge
intensity (10^15 phs sr^-1 nm^-1 m^-2 s^-1)
wavelength (nm)
388.9 nm (2³S–3³P)
501.6 nm (2¹S–3¹P)
587.6 nm (2³P–3³D)
667.8 nm (2¹P–3¹D)
706.5 nm (2³P–3³S)
728.1 nm (2¹P–3¹S)

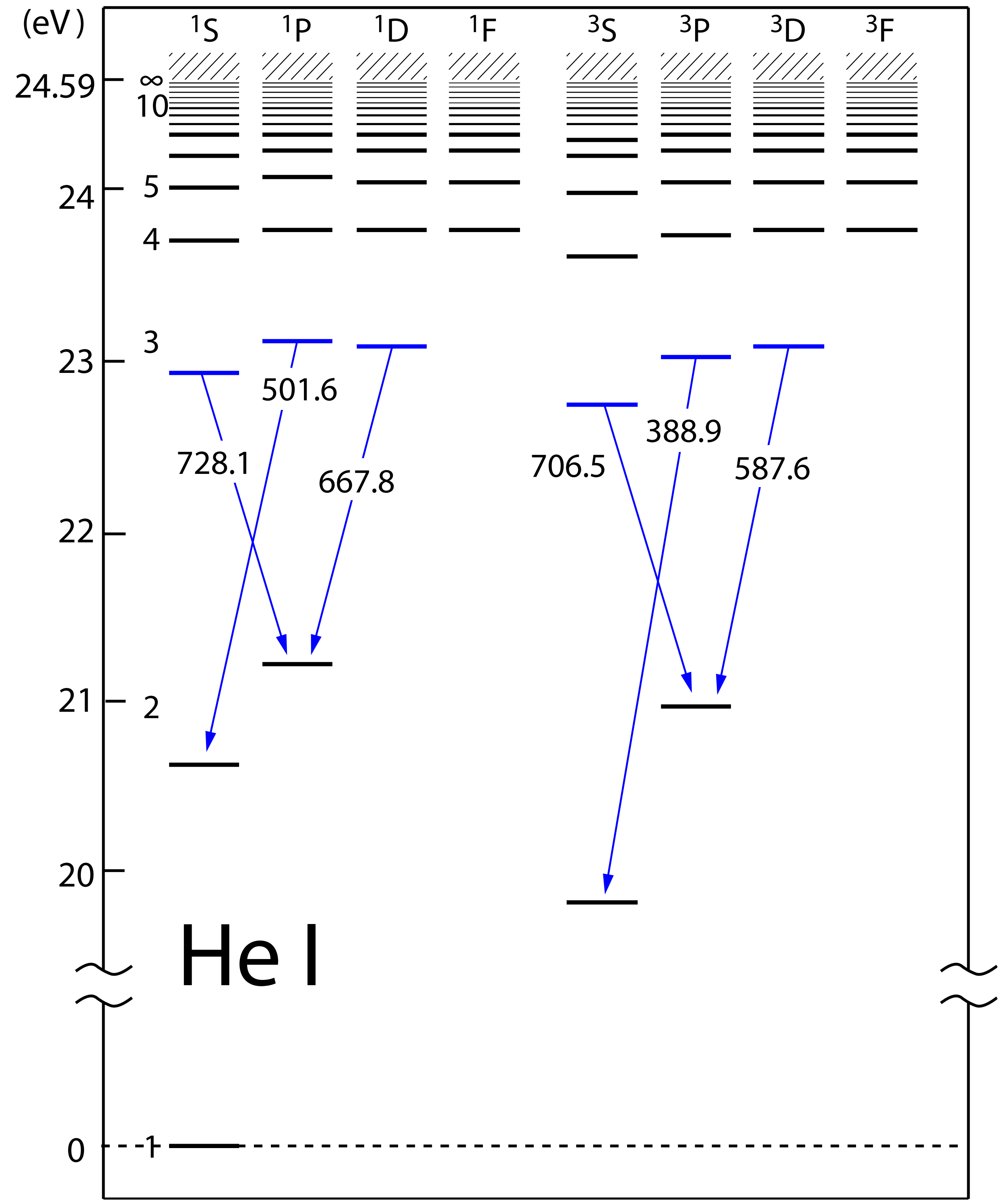
(eV)
¹S ¹P ¹D ¹F ³S ³P ³D ³F
24.59
728.1
501.6
667.8
706.5
388.9
587.6
He I

corona equilibrium

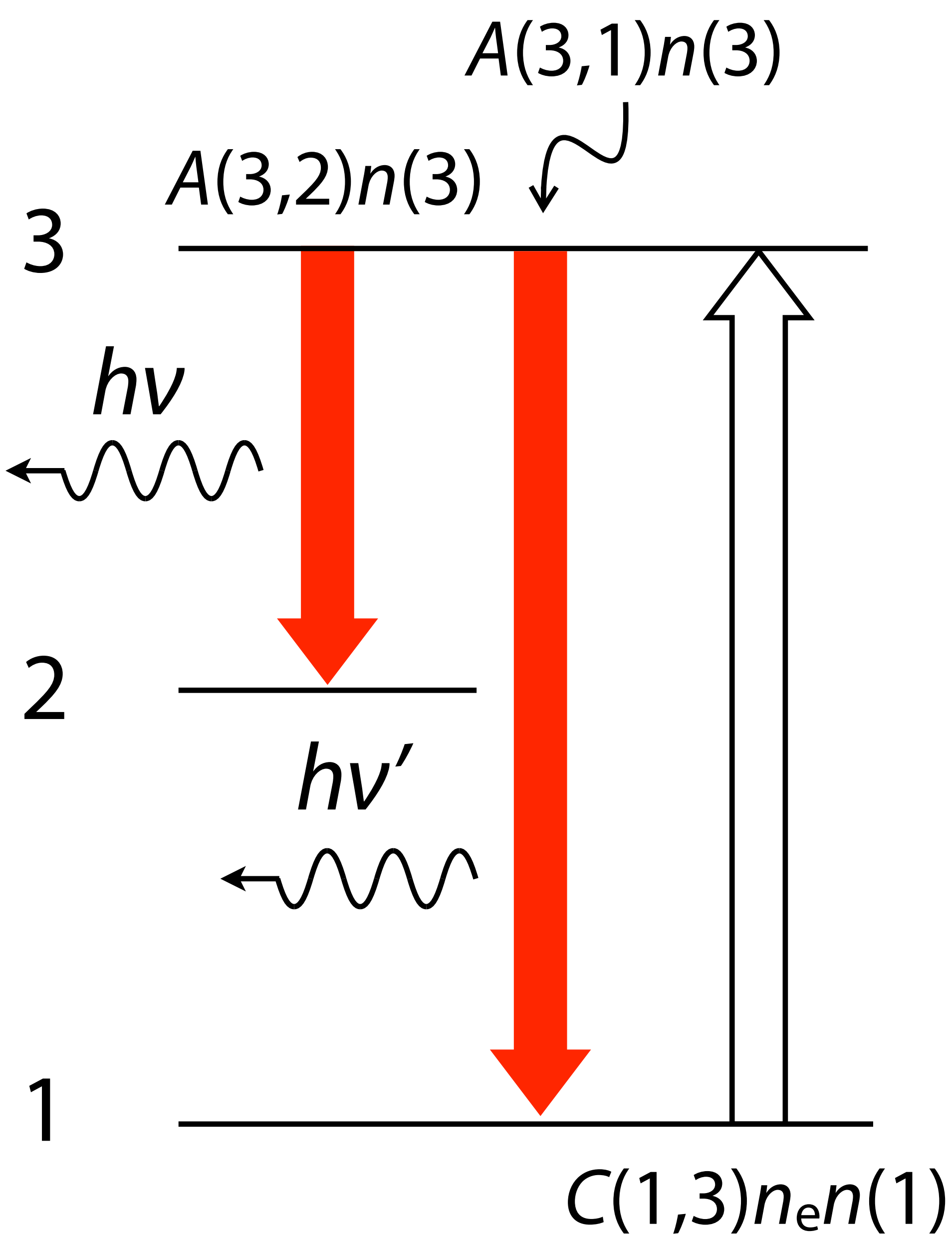

$$C(1,3)n_e n(1) = [A(3,1) + A(3,2)]n(3)$$

more generally

$$C(1,p)n_e n(1) = \sum_{q<p} A(p,q)n(p)$$

$$n(p) = \frac{C(1,p)n_e}{\sum_{q<p} A(p,q)} n(1)$$

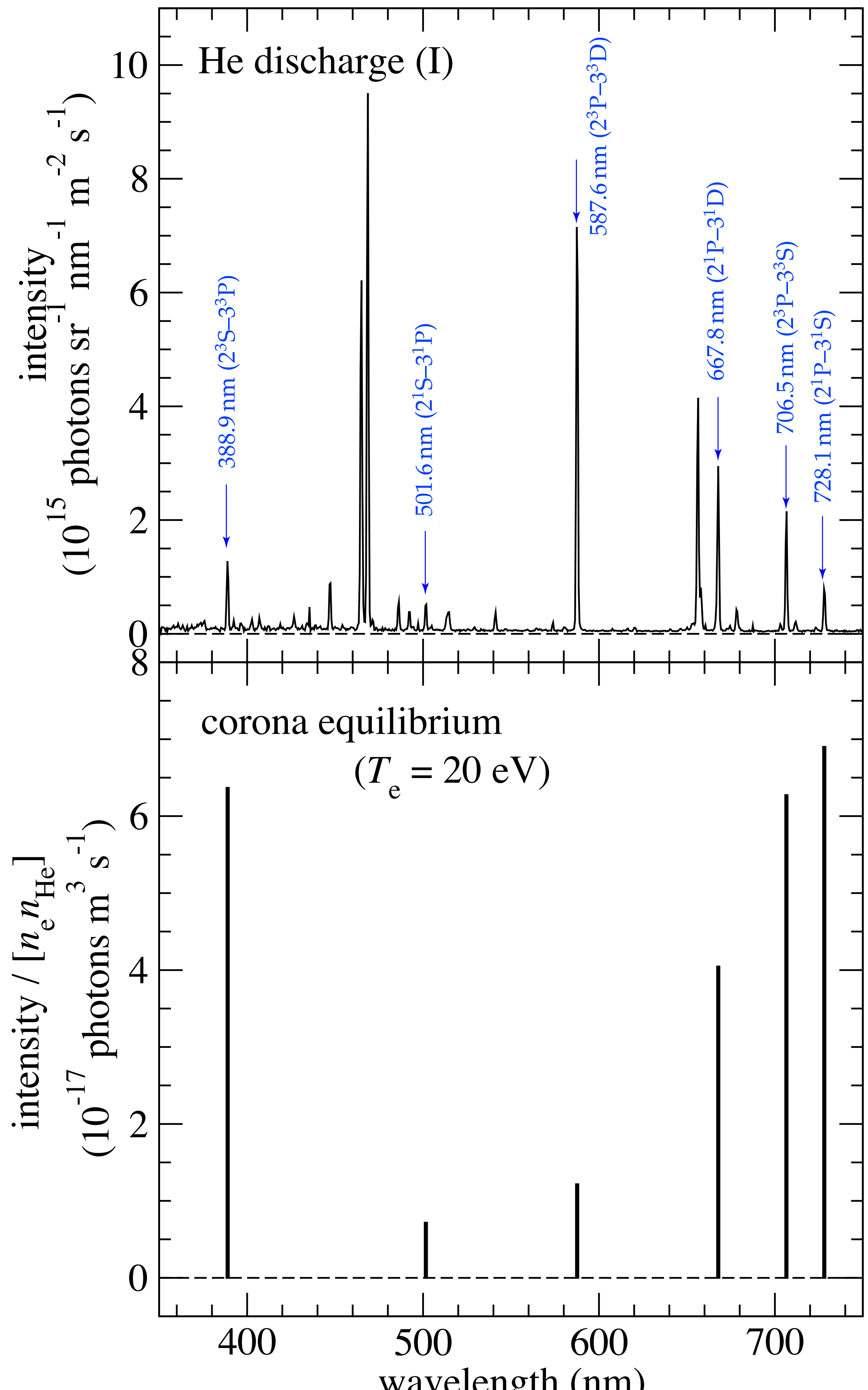

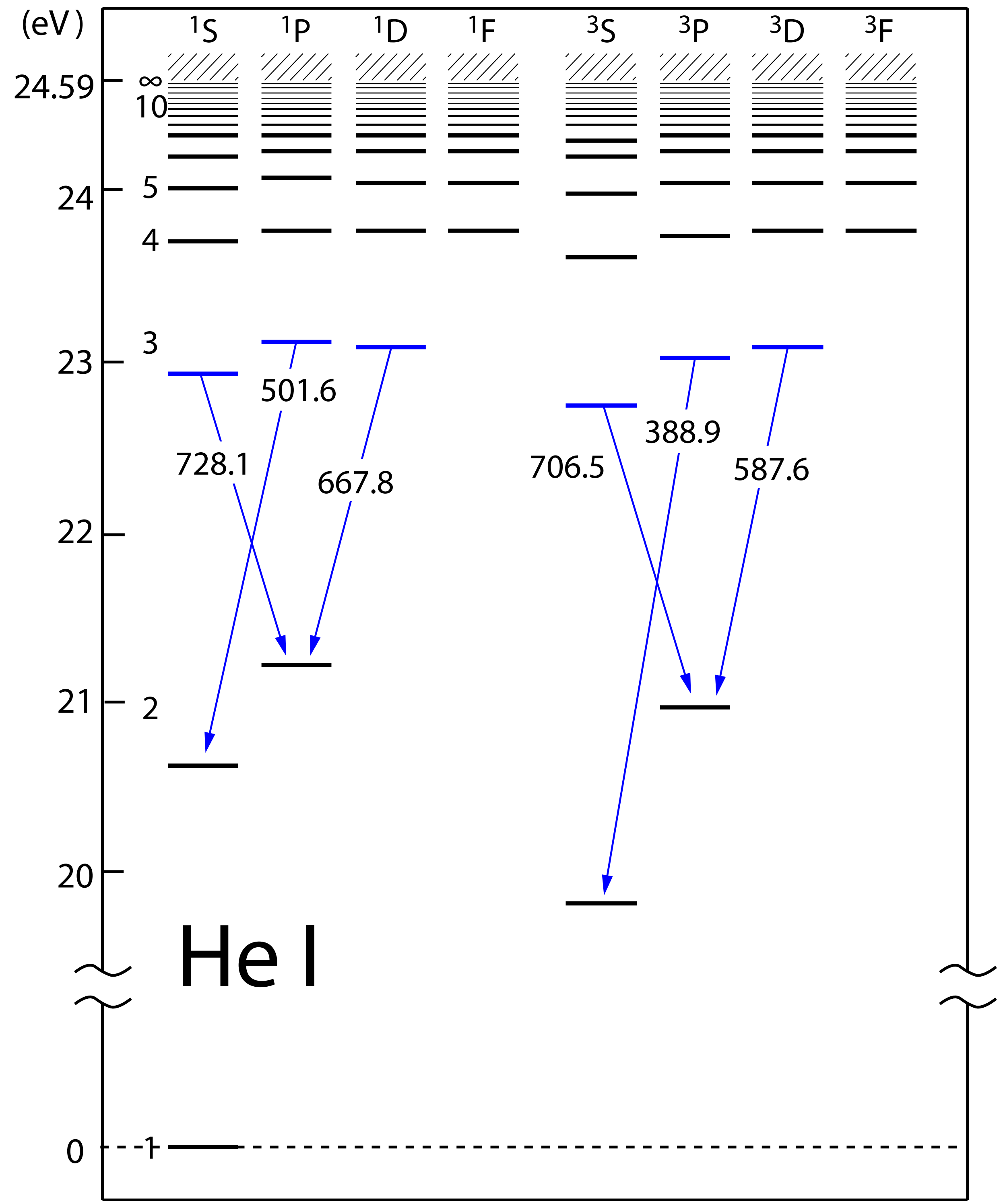

corona model cannot explain
observation results

Phase I

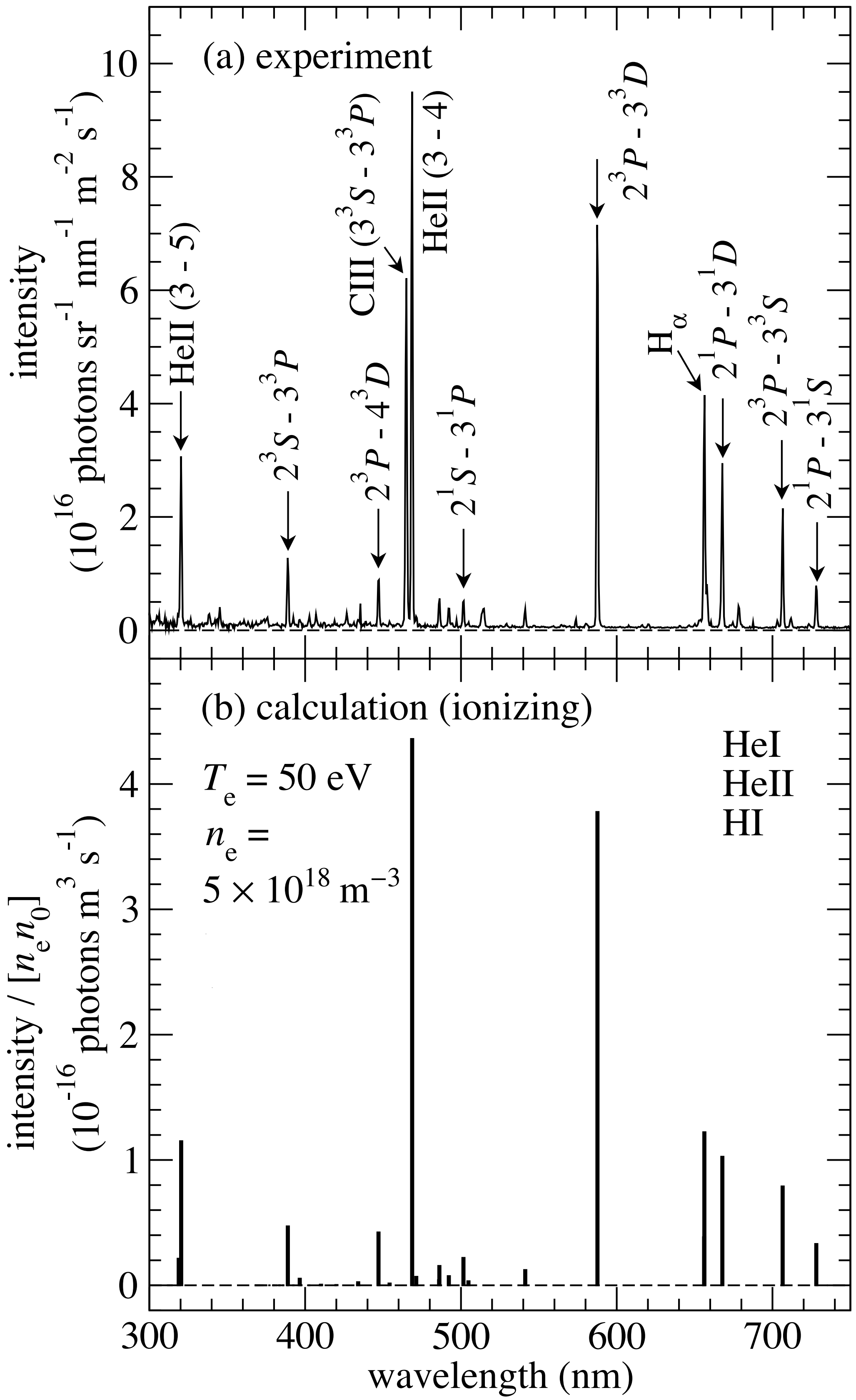

$$n(p) = r_1(p) n_e n(1)$$

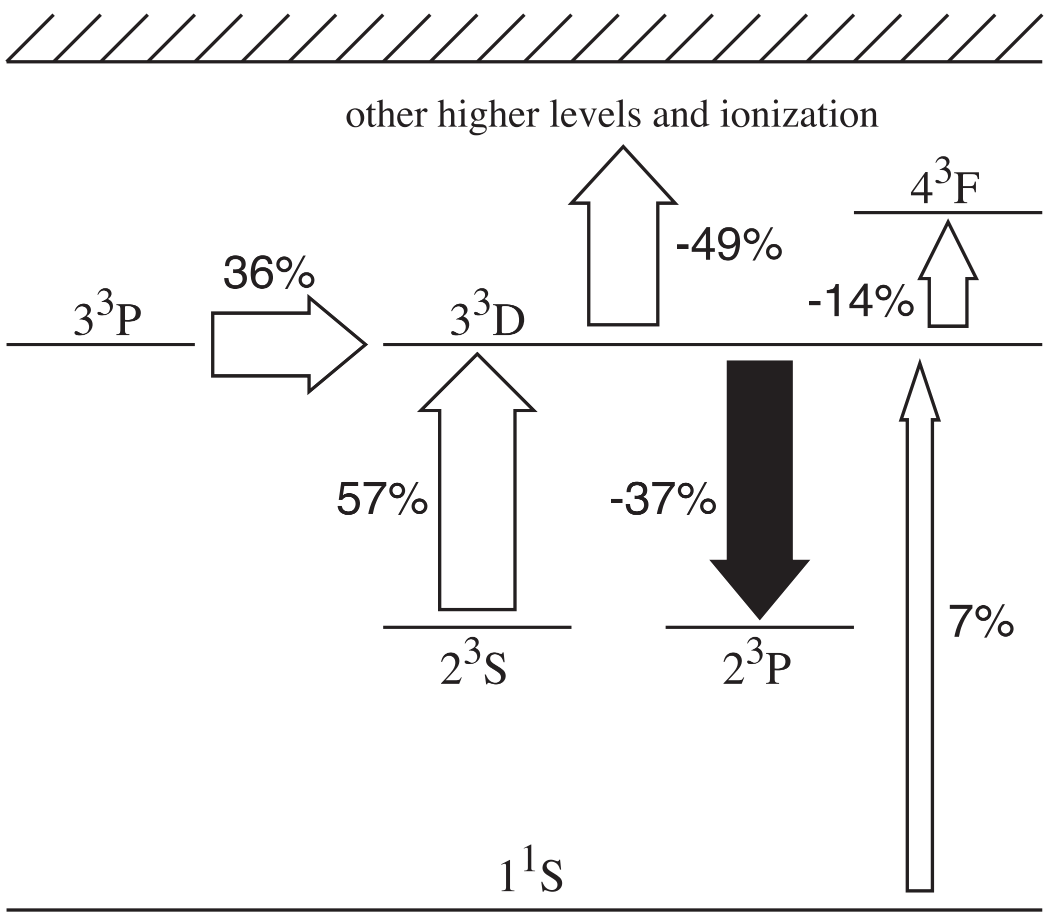

Phase III

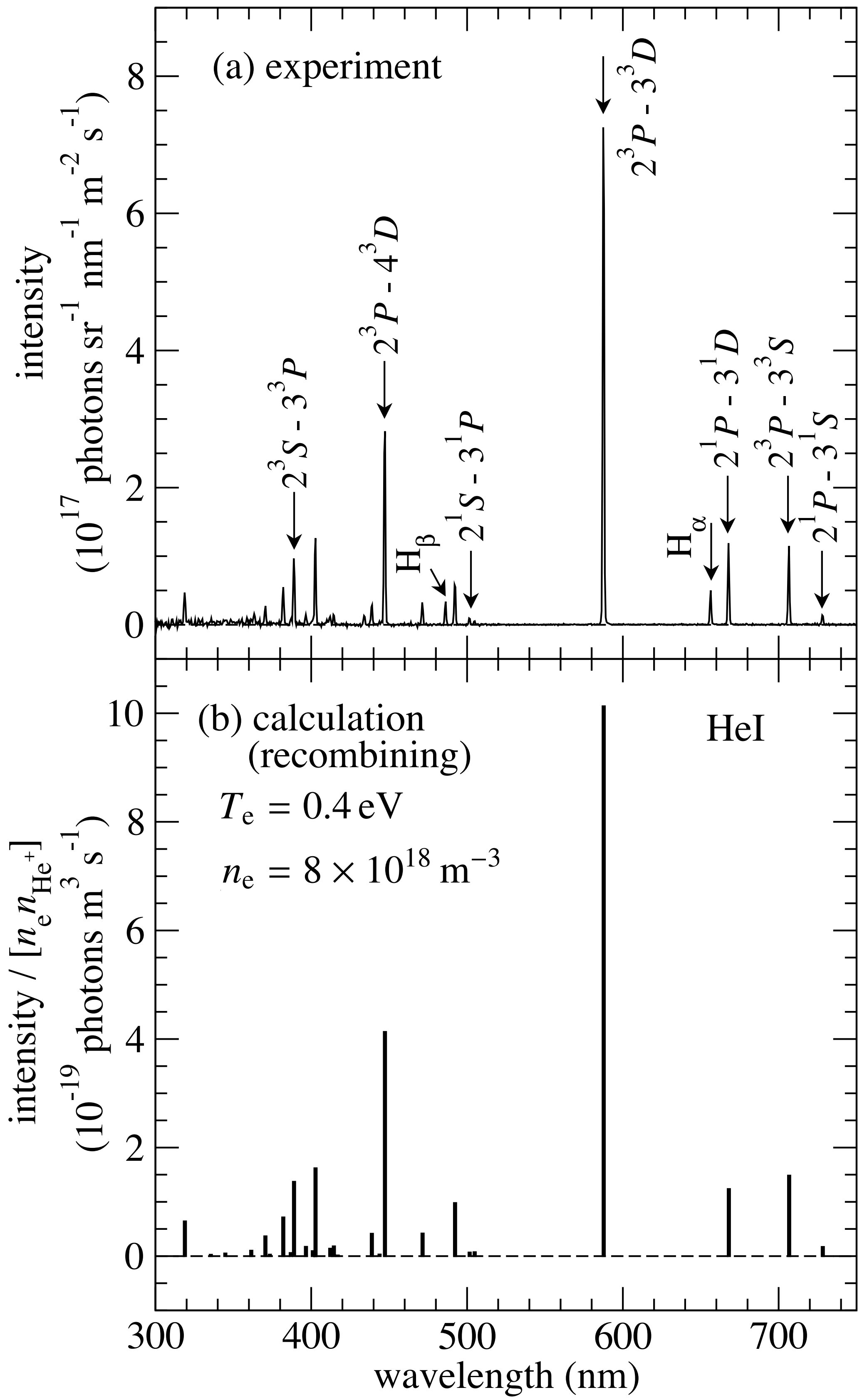

$$n(p) = r_0(p) n_e n_i$$

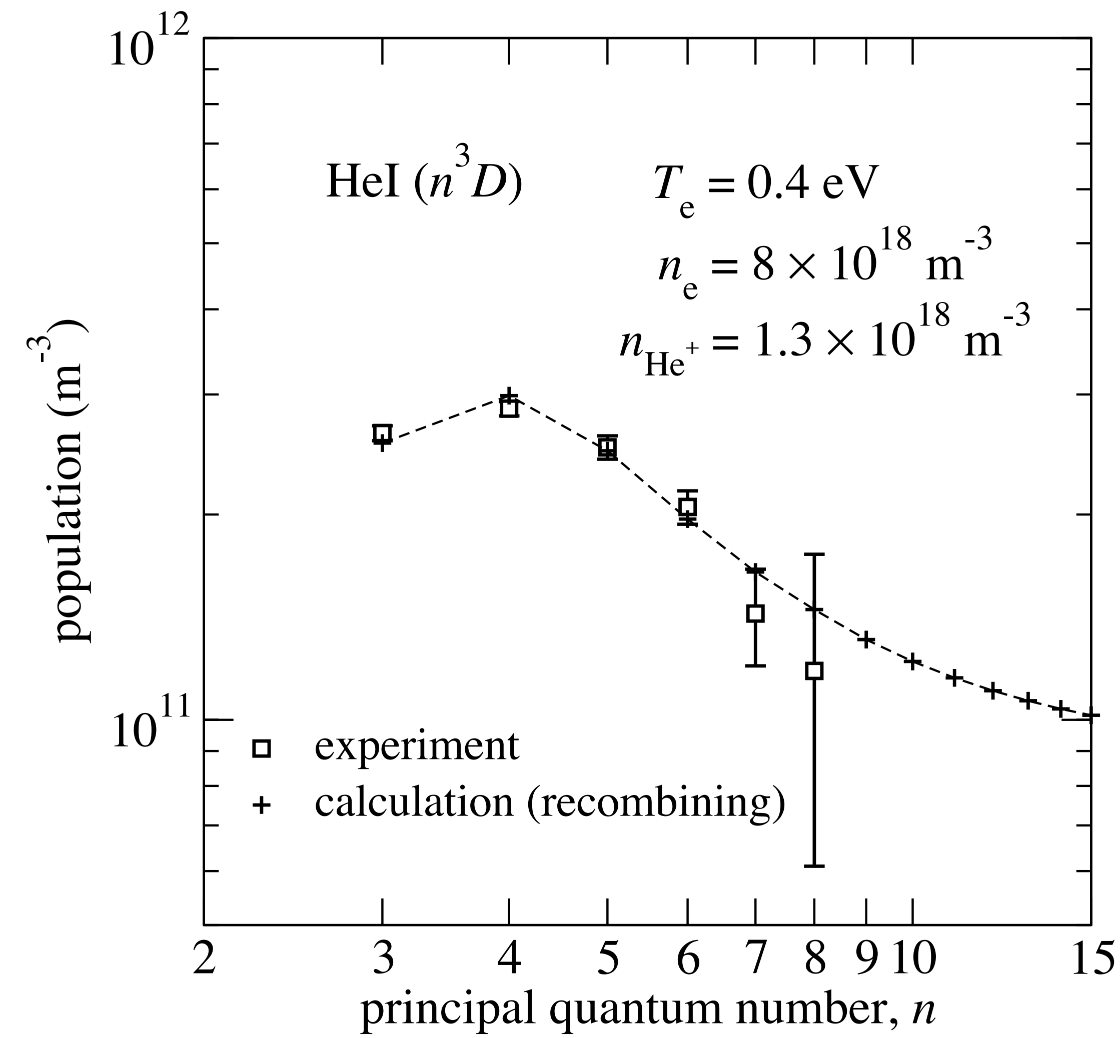

Phase II

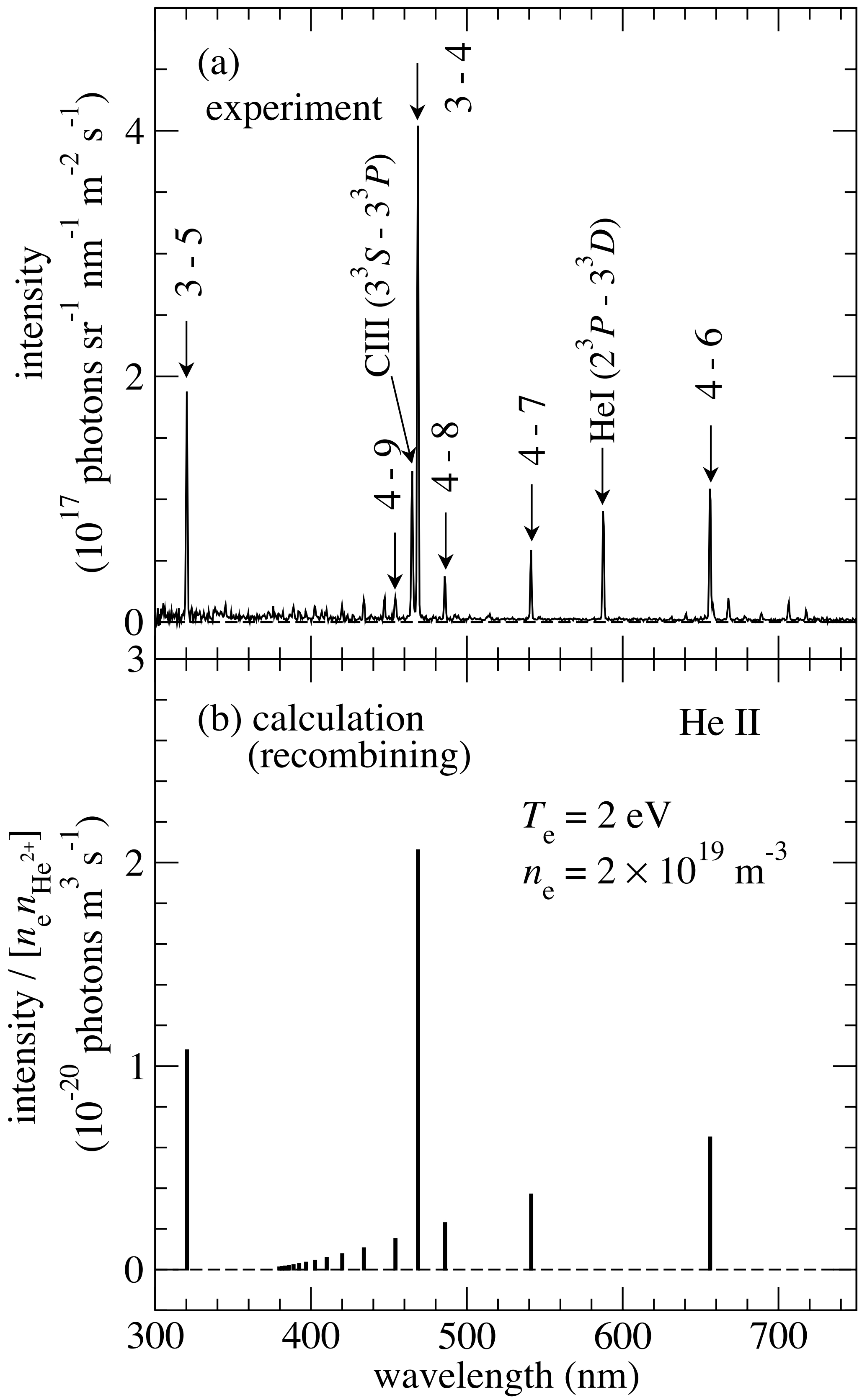

- recombining plasma of HeII appears earlier than HeI
- derived T_e is higher

- spectroscopy is a fundamental diagnostic method for fusion plasmas

- collisional-radiative model is essential for analyzing measured line intensities

T_e and n_e analysis with helium lines

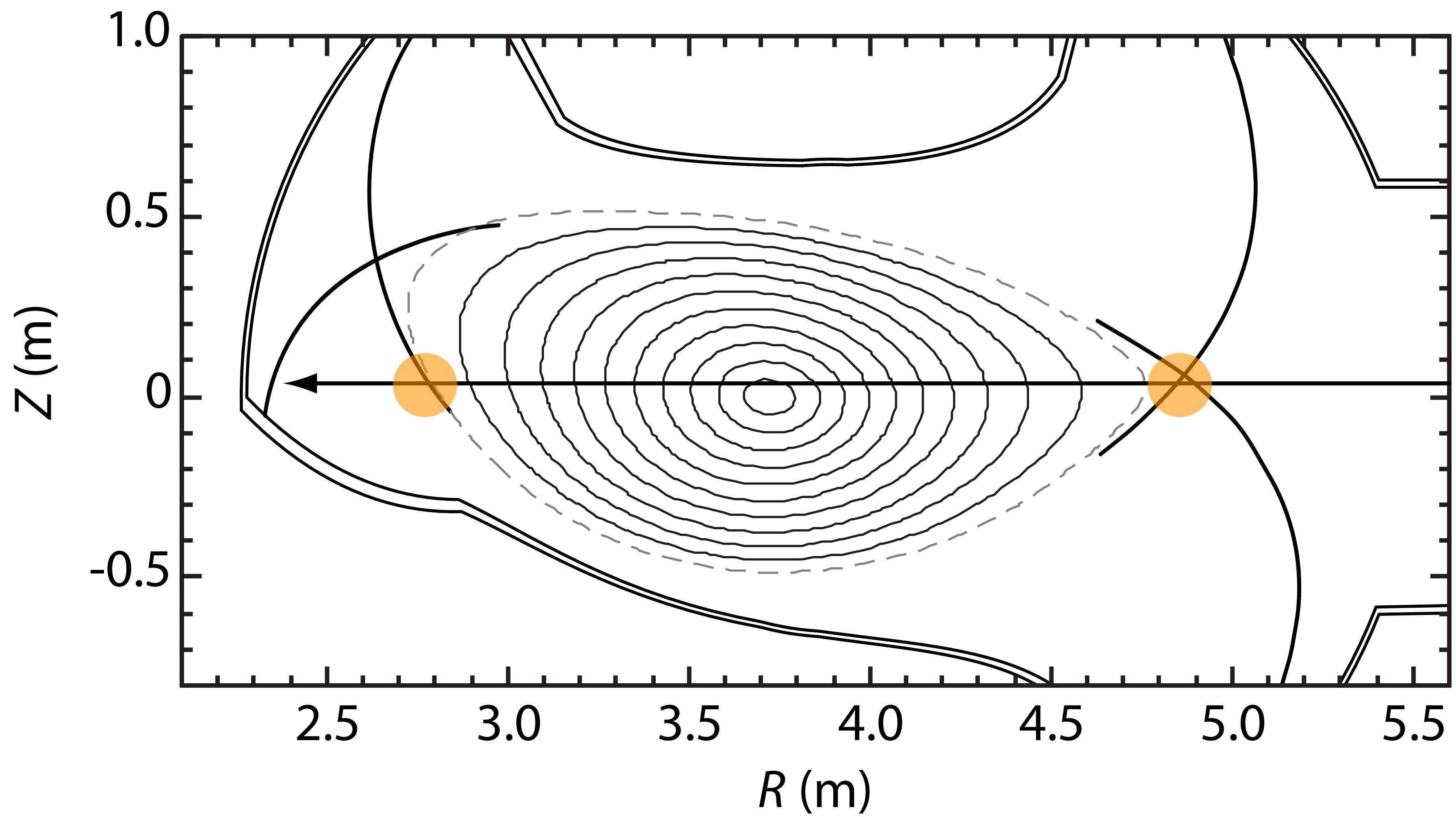

- measurement has been made with single collimated line-of-sight
- dominant line emission is known to be localized at edge region

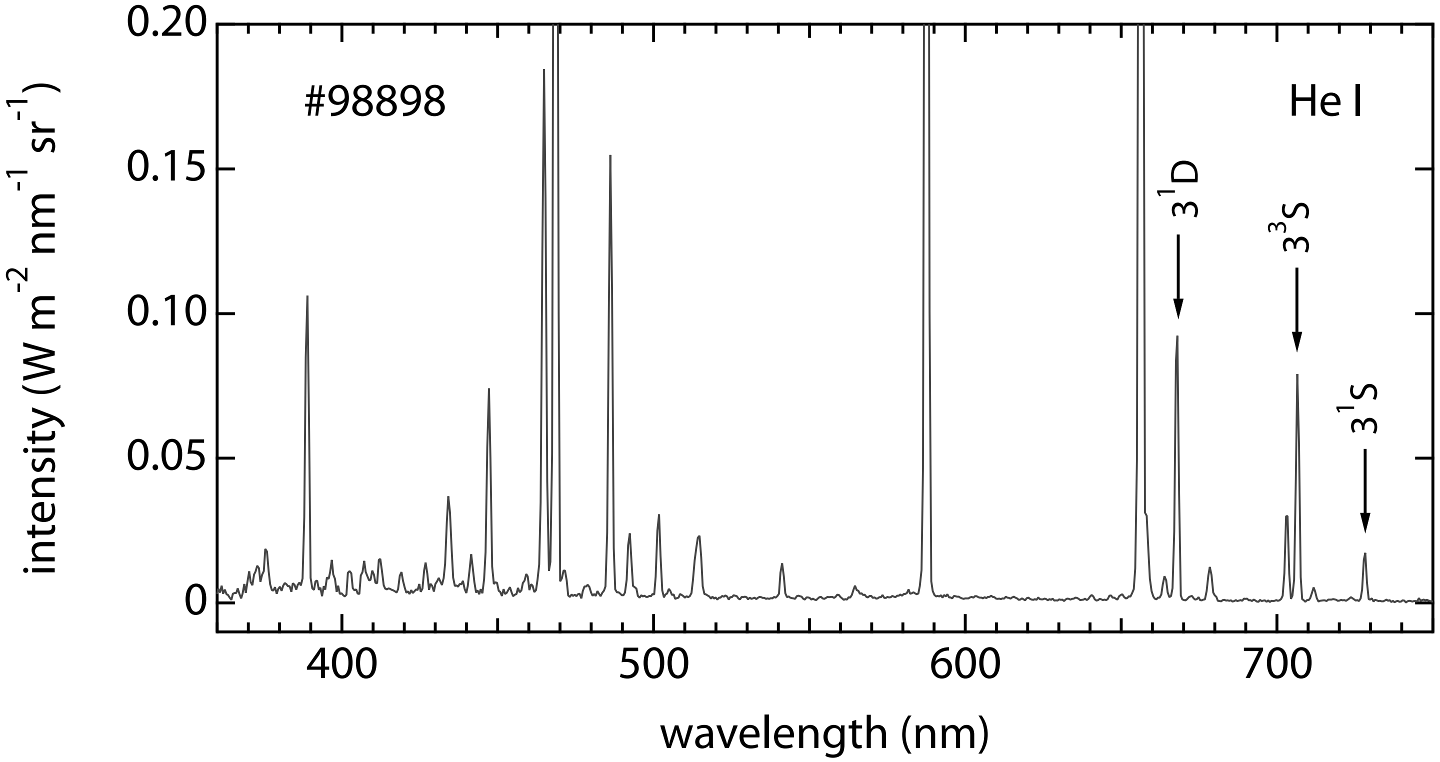

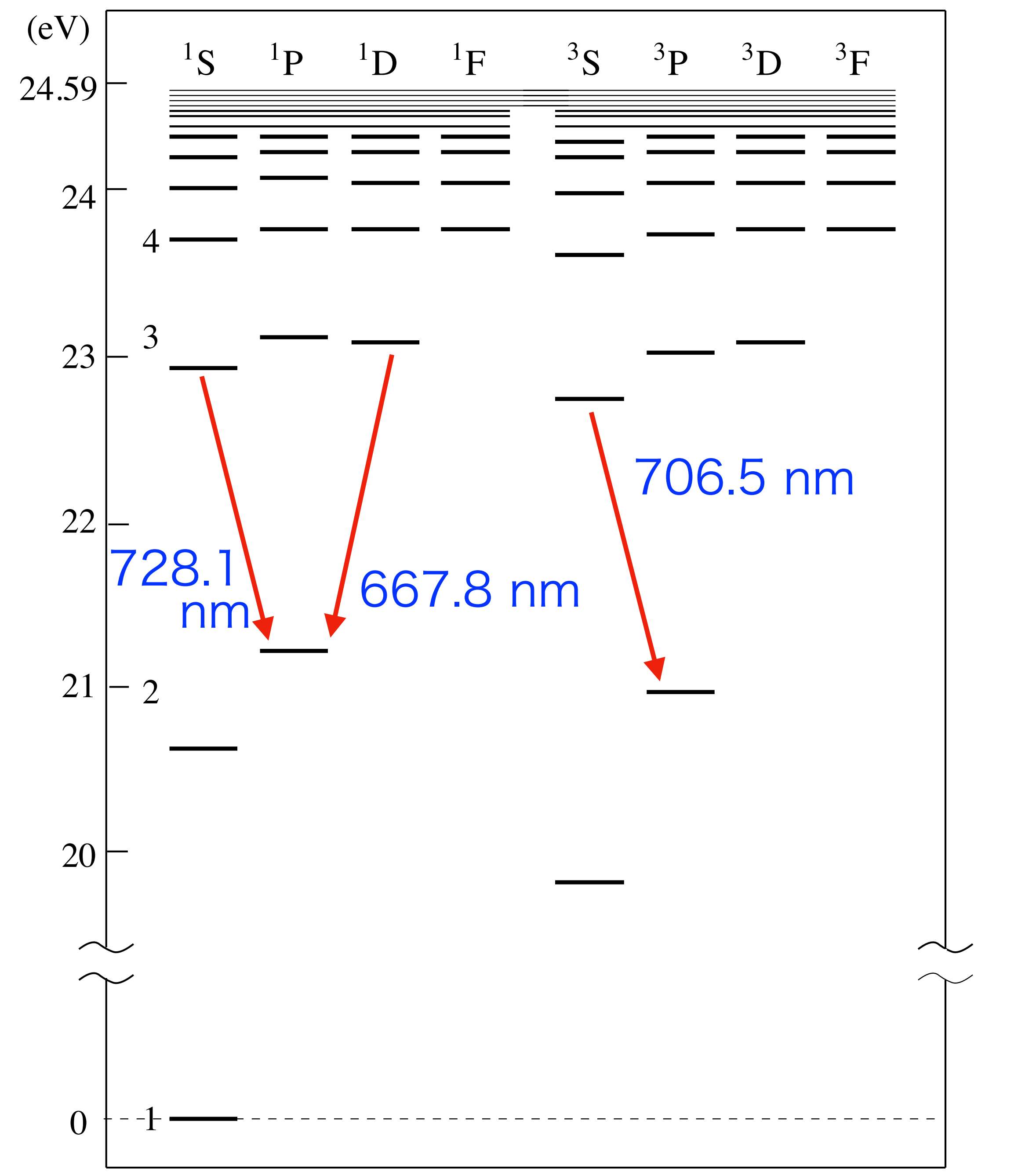

- we first focus on the ratios of three emission lines which are known to have large dependence on T_e or n_e

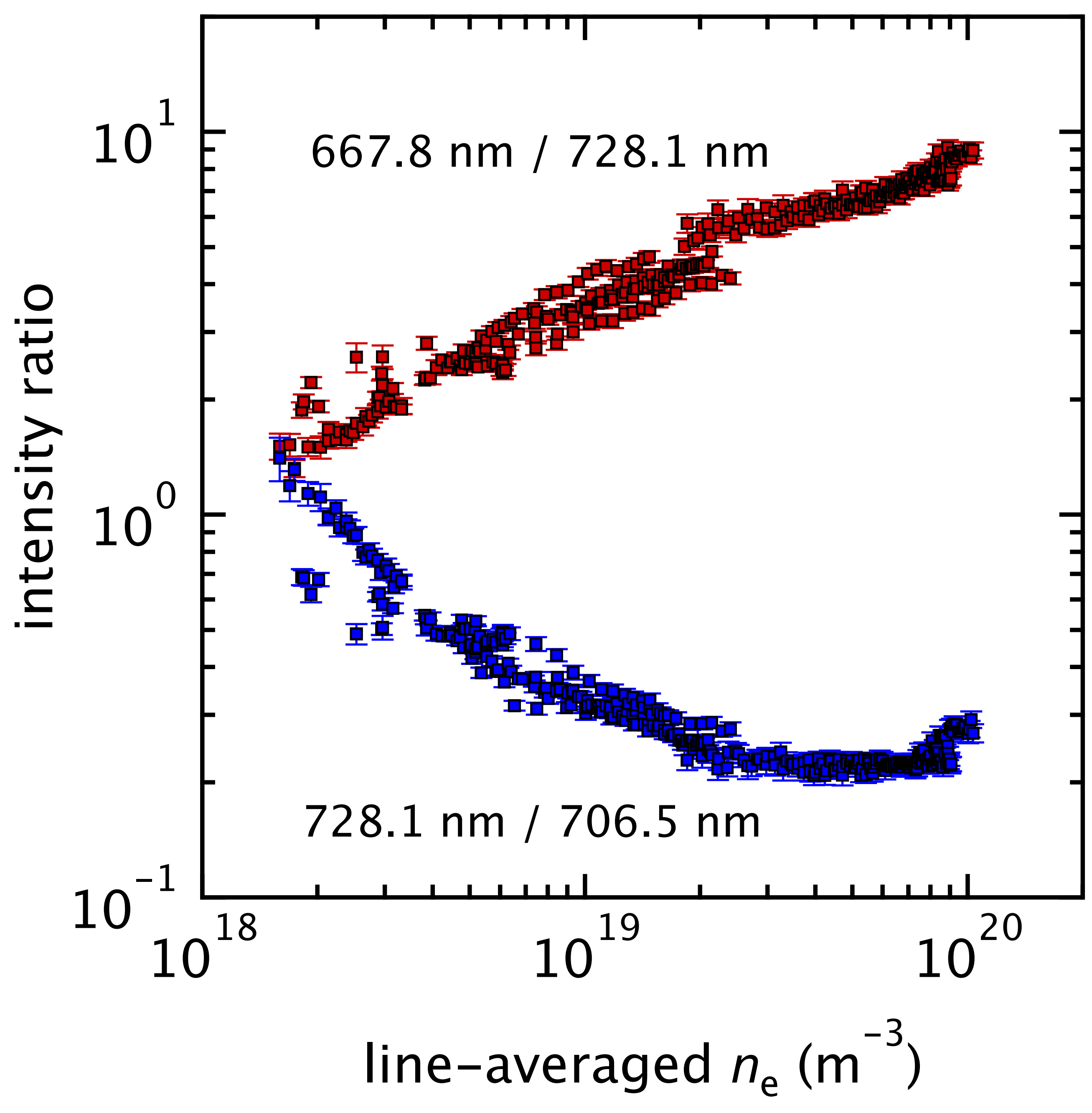

667.8 nm / 728.1 nm
728.1 nm / 706.5 nm
intensity ratio
line-averaged n_e (m^{-3})
10^1
10^0
10^{-1}
10^{18}
10^{19}
10^{20}

$$f(T_e, n_e) = \sum_p \left(\frac{n_{cal}(p) - n_{mes}(p)}{n_{mes}(p)} \right)^2 \quad \text{with} \quad p \in \{3^1\text{S},\ 3^1\text{D},\ 3^3\text{S}\}$$

- least-squares fitting is attempted with an error function which describes the difference between the model and measurement results

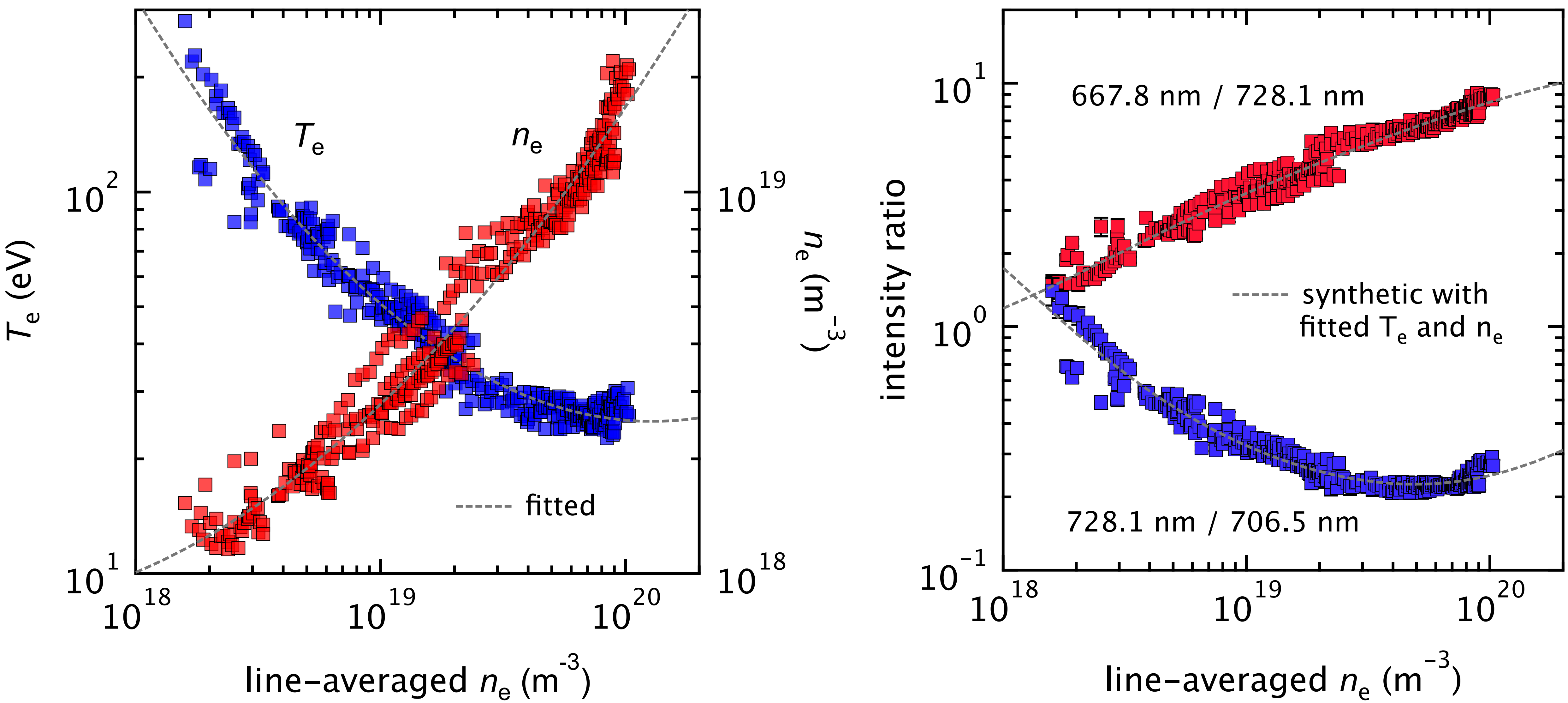

- T_e and n_e derived seem to be reasonable and fitting looks to be going well

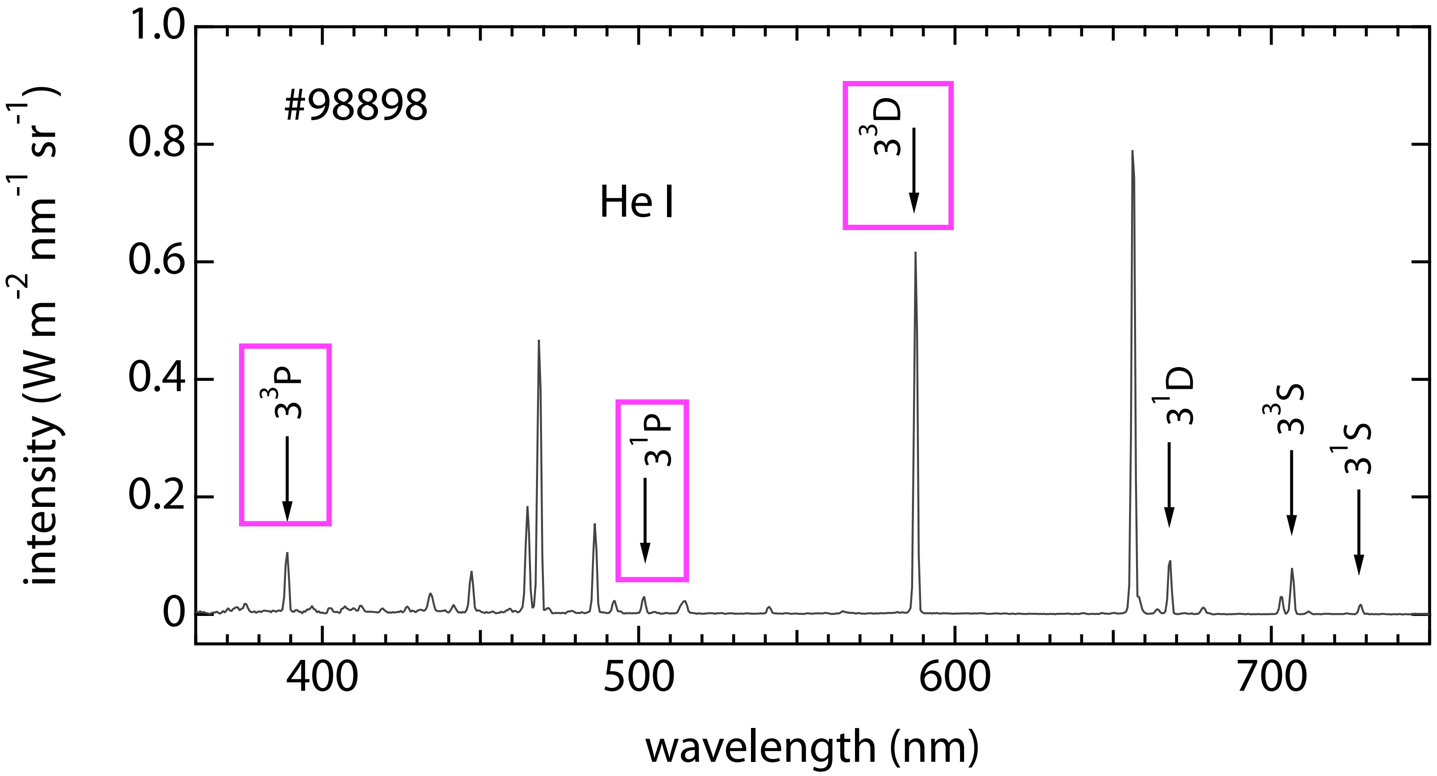

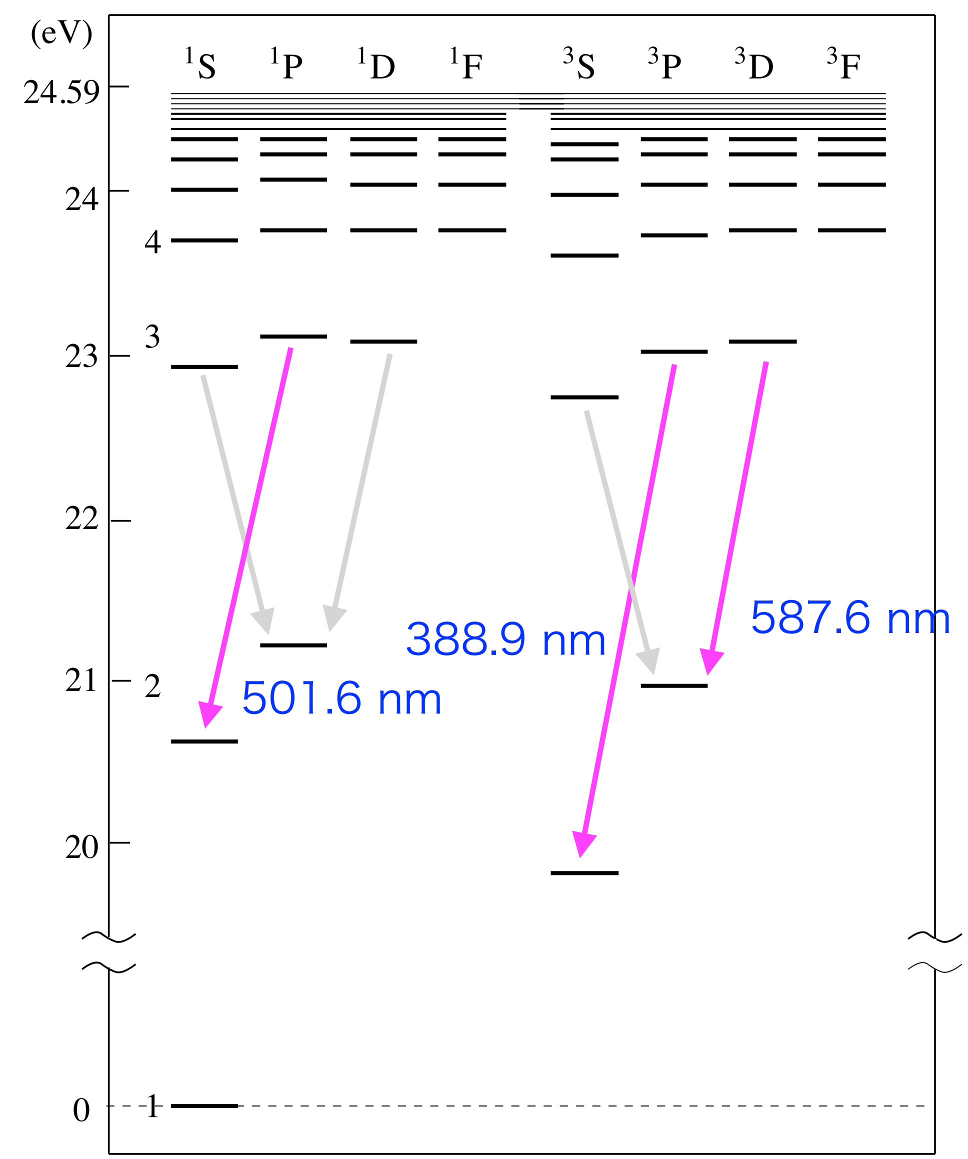

- obtained results are examined with using other lines

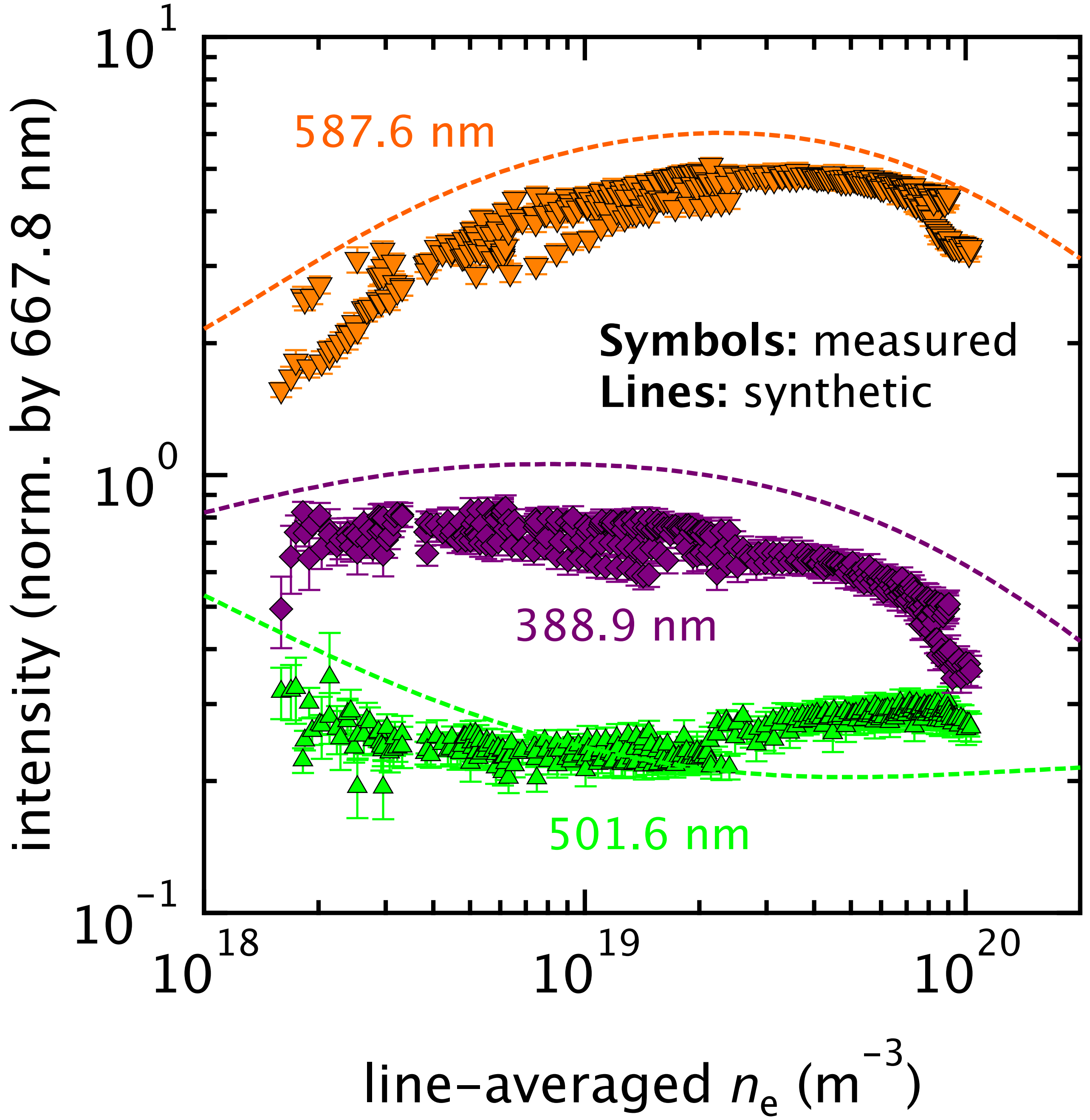

587.6 nm
Symbols: measured
Lines: synthetic
388.9 nm
501.6 nm
intensity (norm. by 667.8 nm)
line-averaged n_e (m^{-3})
10^{1}
10^{0}
10^{-1}
10^{18}
10^{19}
10^{20}

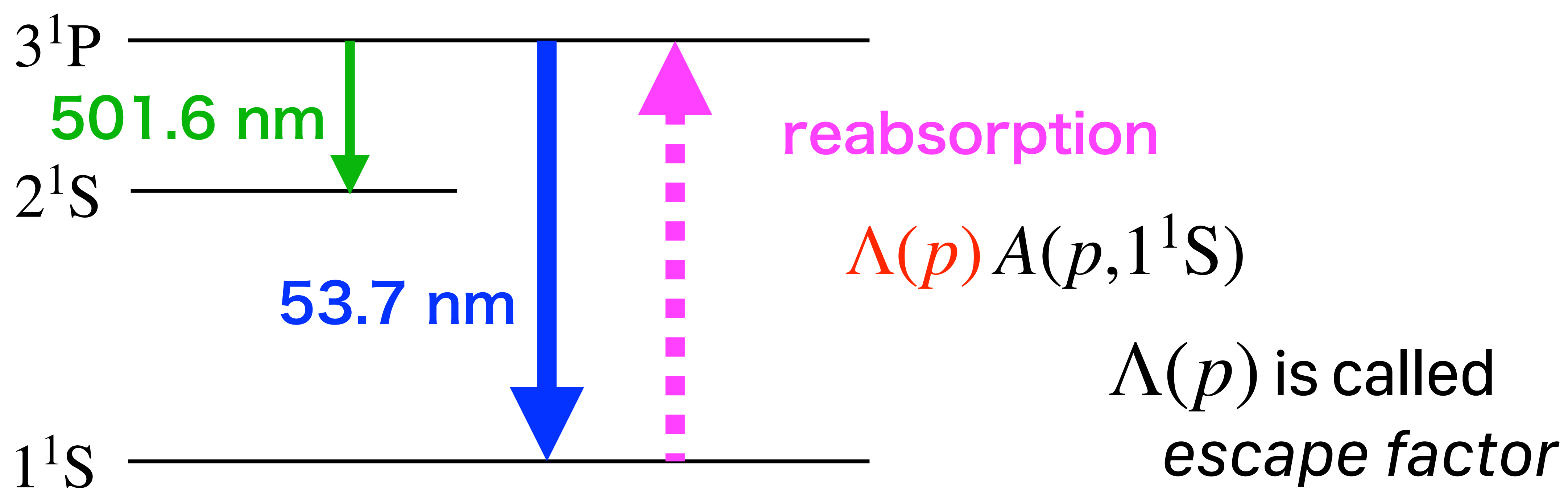

reabsorption effectively works to reduce the transition probability of spontaneous radiative transition and to increase the upper level populations

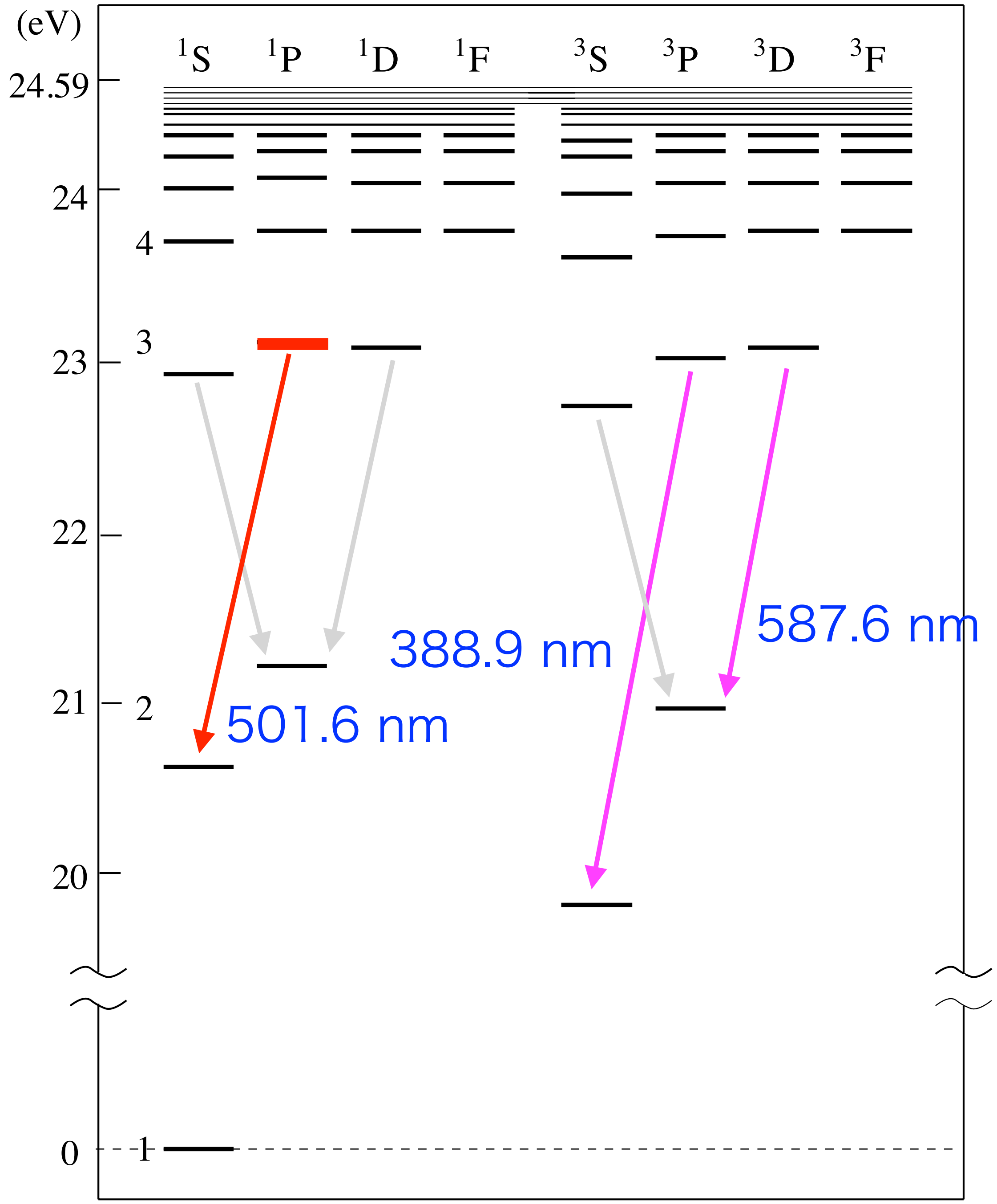

(eV)
¹S ¹P ¹D ¹F ³S ³P ³D ³F
24.59
24
23
22
21
20
0
4
3
2
1
501.6 nm
388.9 nm
587.6 nm

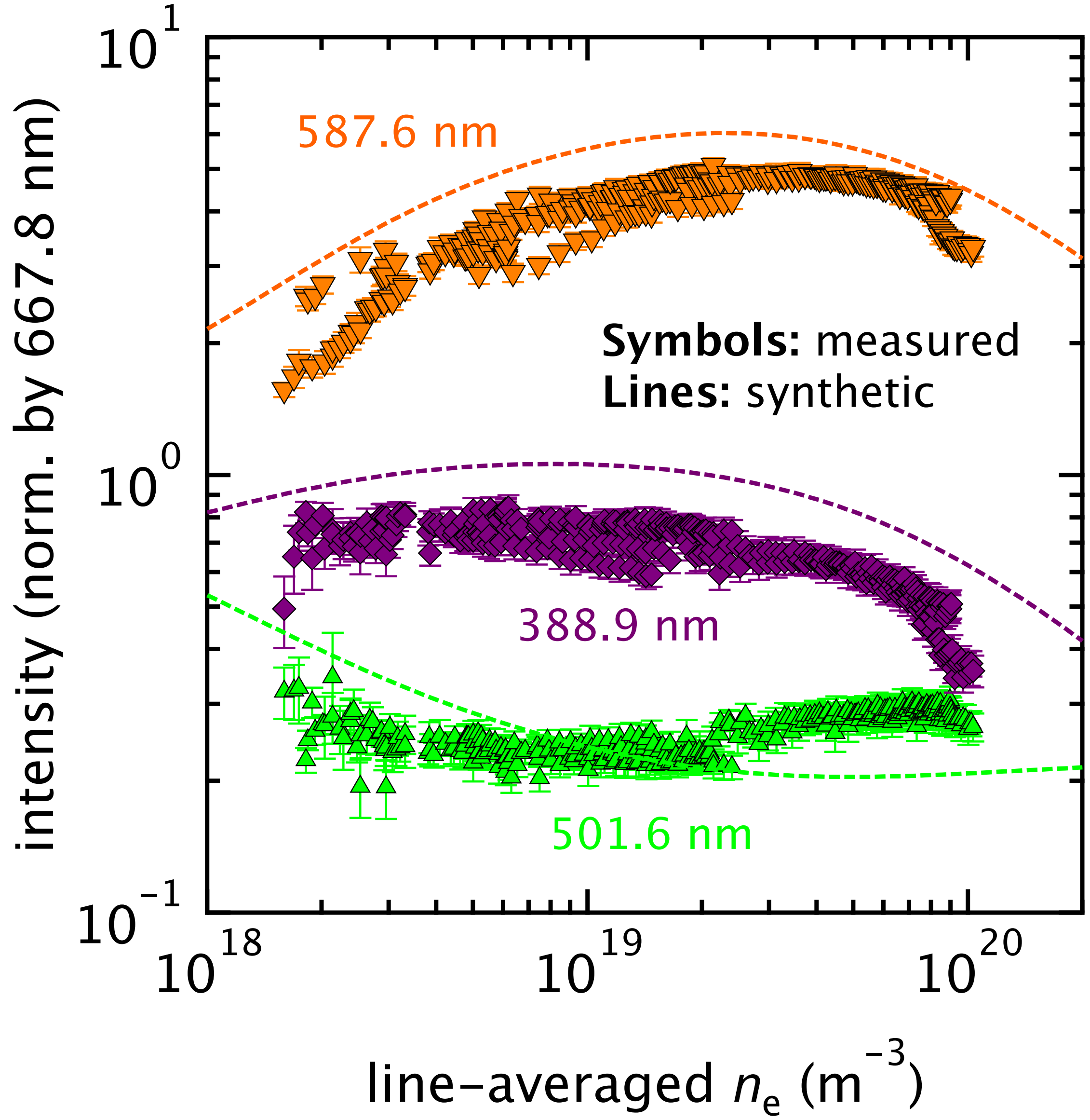

intensity (norm. by 667.8 nm)
line-averaged n_e (m^{-3})
10^{1}
10^{0}
10^{-1}
10^{18}
10^{19}
10^{20}
587.6 nm
388.9 nm
501.6 nm
Symbols: measured
Lines: synthetic

$$f(T_\mathrm{e}, n_\mathrm{e}, \Lambda(2^1\mathrm{P}), \Lambda(3^1\mathrm{P}), \ldots) = \Sigma_p \left(\frac{n(p) - n_\mathrm{mes}(p)}{n_\mathrm{mes}(p)} \right)^2$$

- accurate evaluation of escape factors is difficult
- one idea is to include the escape factors in the fitting parameters, but restrictions should be given for the escape factors

- escape factors can be theoretically evaluated for some simplified geometries such as slab or cylindrical structures

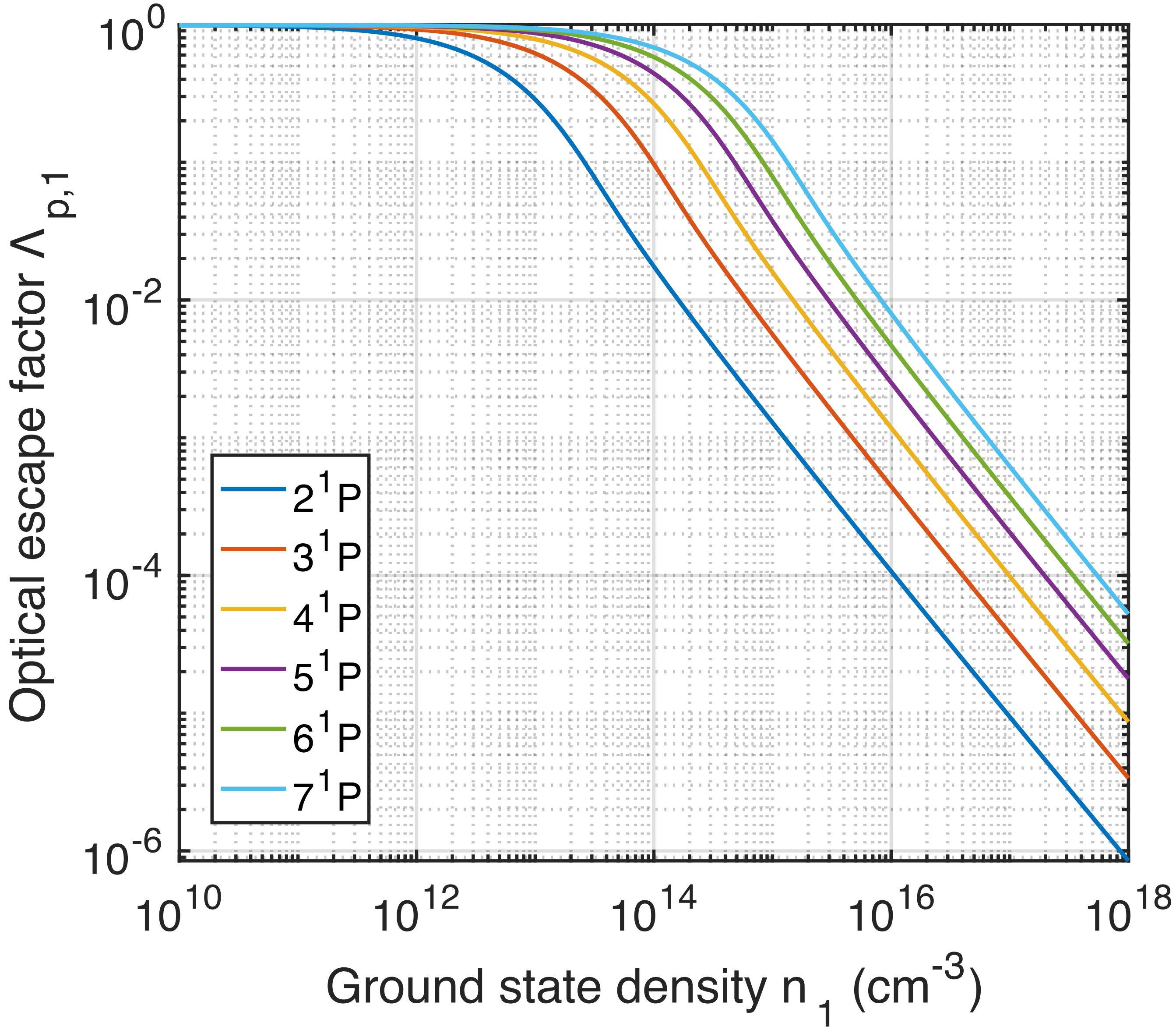

slab with 1 cm thickness

- restriction is added as a regularization term to the error function

$$f\left(T_{\mathrm{e}}, n_{\mathrm{e}}, \Lambda(2^1\mathrm{P}), \Lambda(3^1\mathrm{P}), \ldots\right) = \frac{1}{N_p}\sum_{p}\left(\frac{n(p) - n_{\mathrm{mes}}(p)}{n_{\mathrm{mes}}(p)}\right)^2 + \mu\frac{1}{N_q}\sum_{q}\left(\frac{\Lambda(q) - \Lambda^{\mathrm{slab}}(q)}{\Lambda^{\mathrm{slab}}(q)}\right)$$

with $p \in \{\text{all upper levels}\}$, $q \in \{n^1\mathrm{P}\}$, and hyperparameter μ

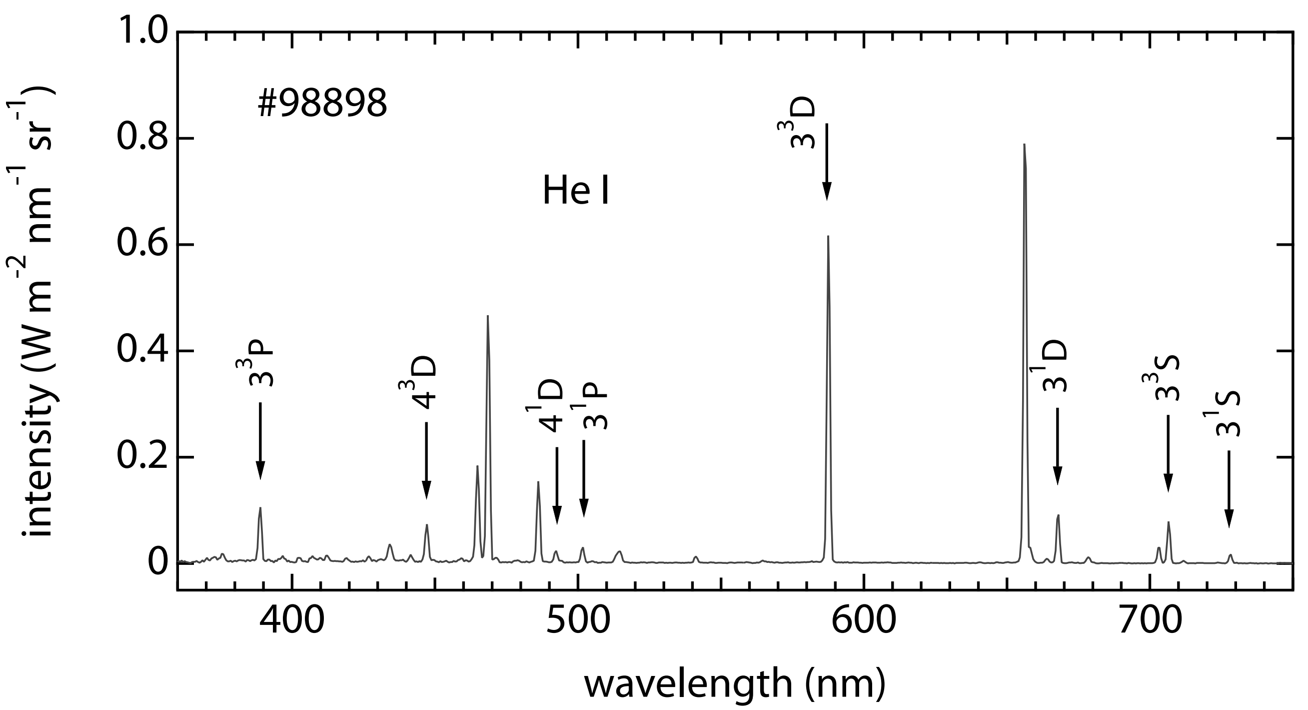

intensity (W m-2 nm-1 sr-1)
wavelength (nm)
#98898
He I
3 3P
4 3D
4 1D
3 1P
3 3D
3 1D
3 3S
3 1S
1.0
0.8
0.6
0.4
0.2
0
400
500
600
700

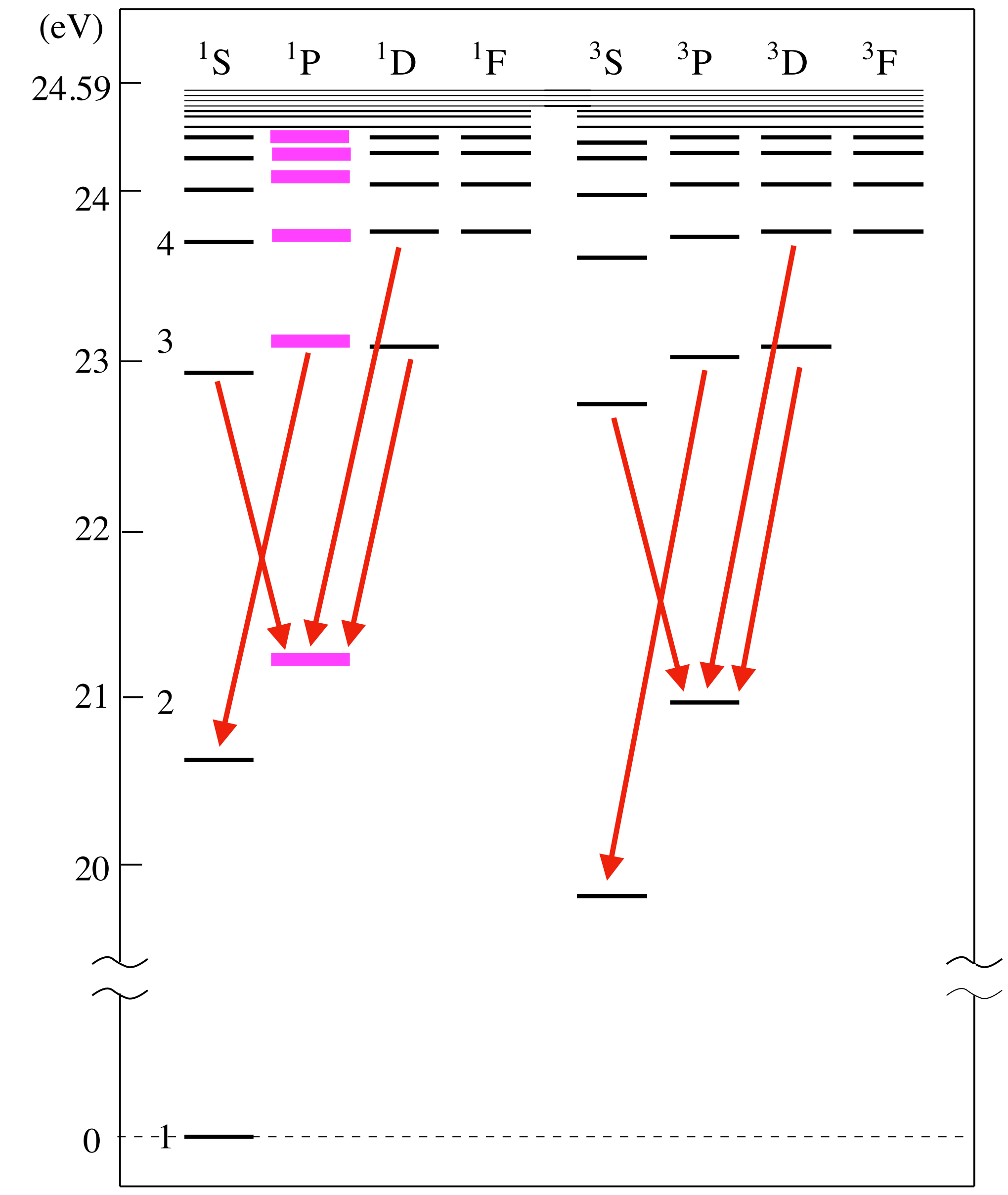

(eV)
24.59
24
23
22
21
20
0
1S
1P
1D
1F
3S
3P
3D
3F
4
3
2
1

- optimizations for the hyper parameter μ and for the number of escape factors considered in the error function are attempted through bias-variance analyses

$$(\text{bias}^2) = \frac{1}{N}\sum_p \left(\frac{\bar{n}_{\text{meas}}(p) - \bar{n}_{\text{fit}}(p)}{\bar{n}_{\text{meas}}(p)} \right)^2$$

$$\text{variance} = \frac{1}{N}\sum_p \left\{ \frac{1}{K}\sum_{k=1}^{K} \left(\frac{\bar{n}_{\text{fit}}(p) - n_{\text{fit}}^{k}(p)}{\bar{n}_{\text{fit}}} \right)^2 \right\}$$

K: number of spectra taken
for the same plasma condition

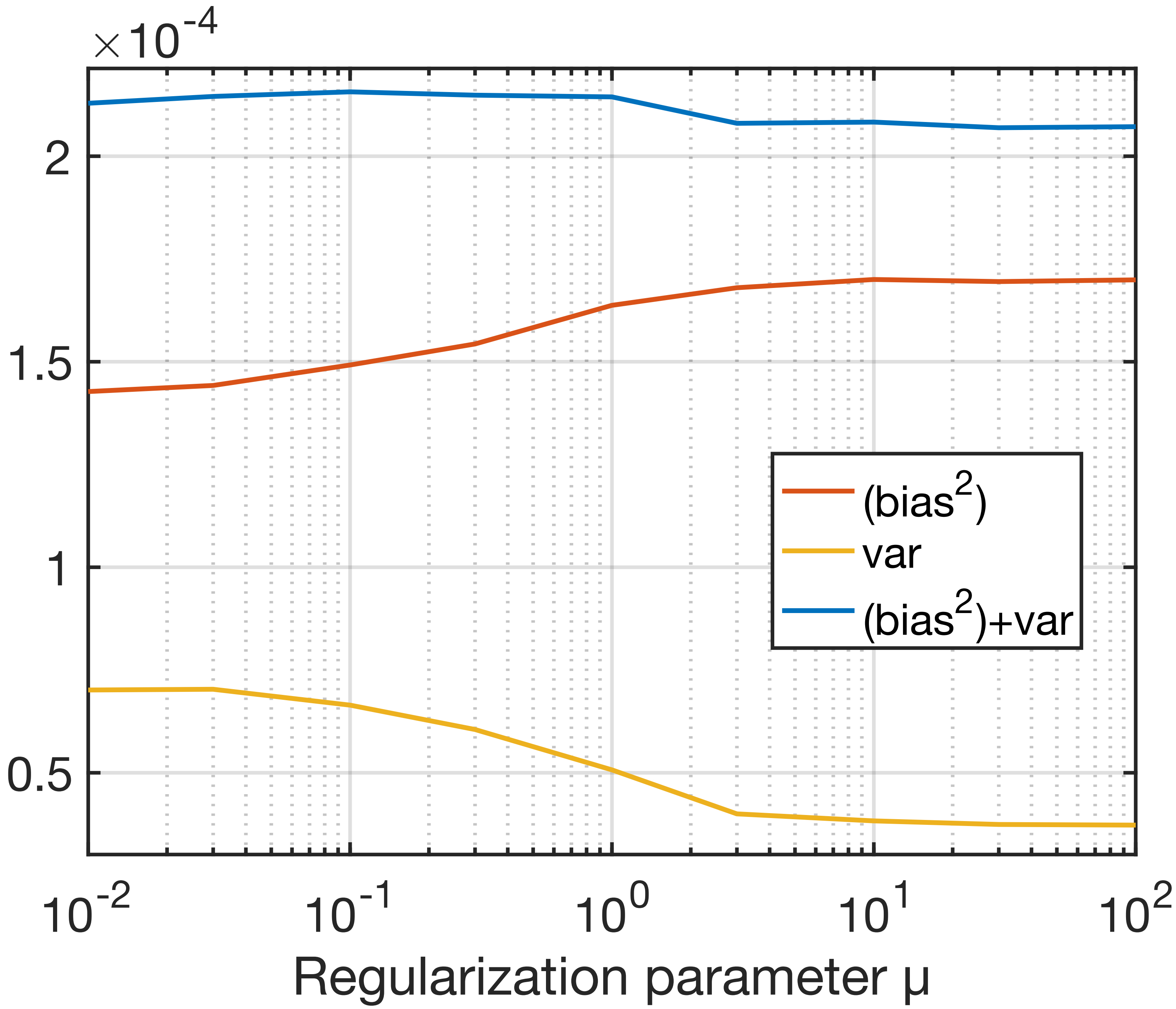

$\times 10^{-4}$
2
1.5
1
0.5
10^{-2}
10^{-1}
10^{0}
10^{1}
10^{2}
Regularization parameter μ
(bias^2)
var
(bias^2)+var

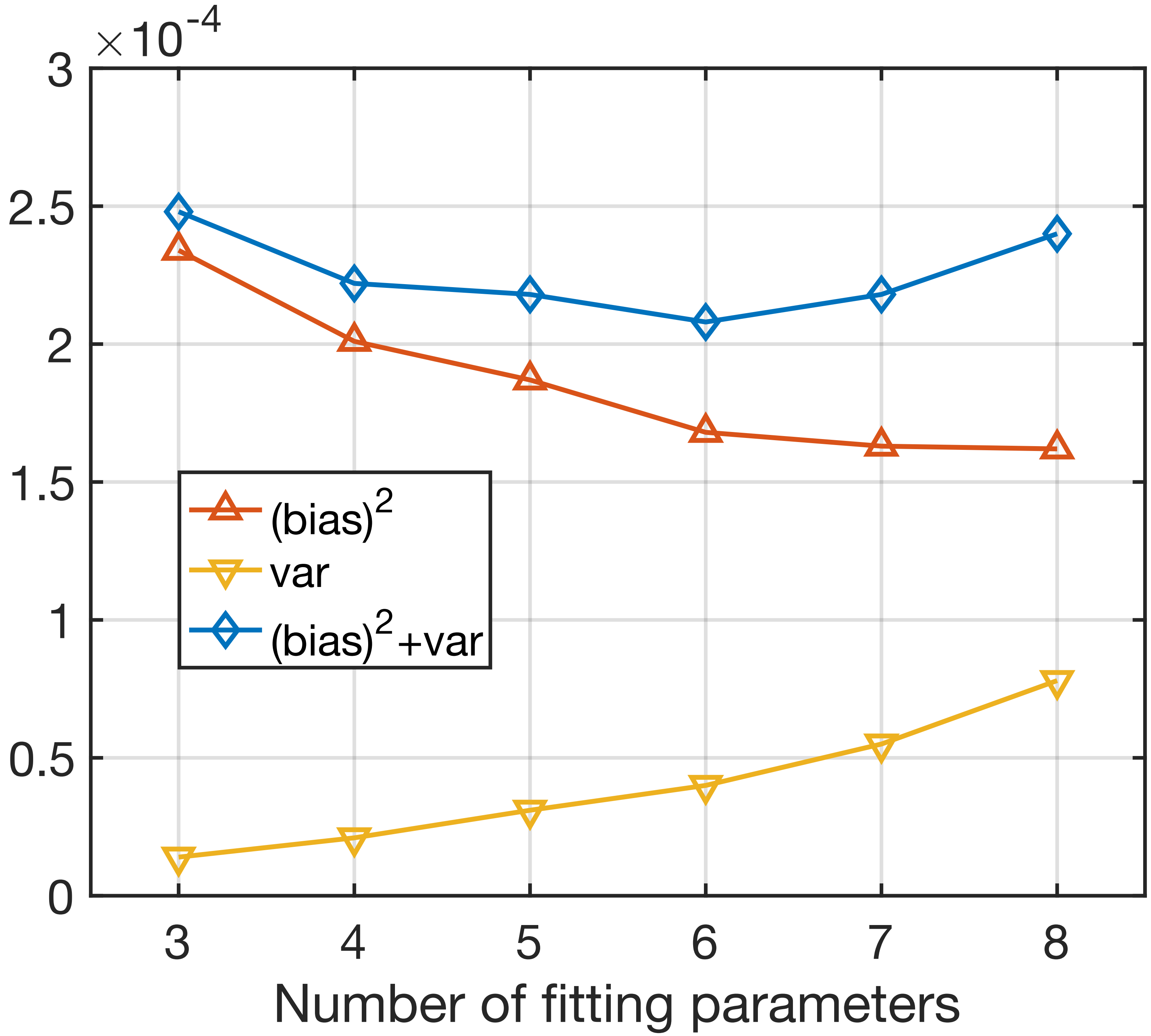

×10^-4
3
2.5
2
1.5
1
0.5
0
(bias)^2
var
(bias)^2+var
3
4
5
6
7
8
Number of fitting parameters

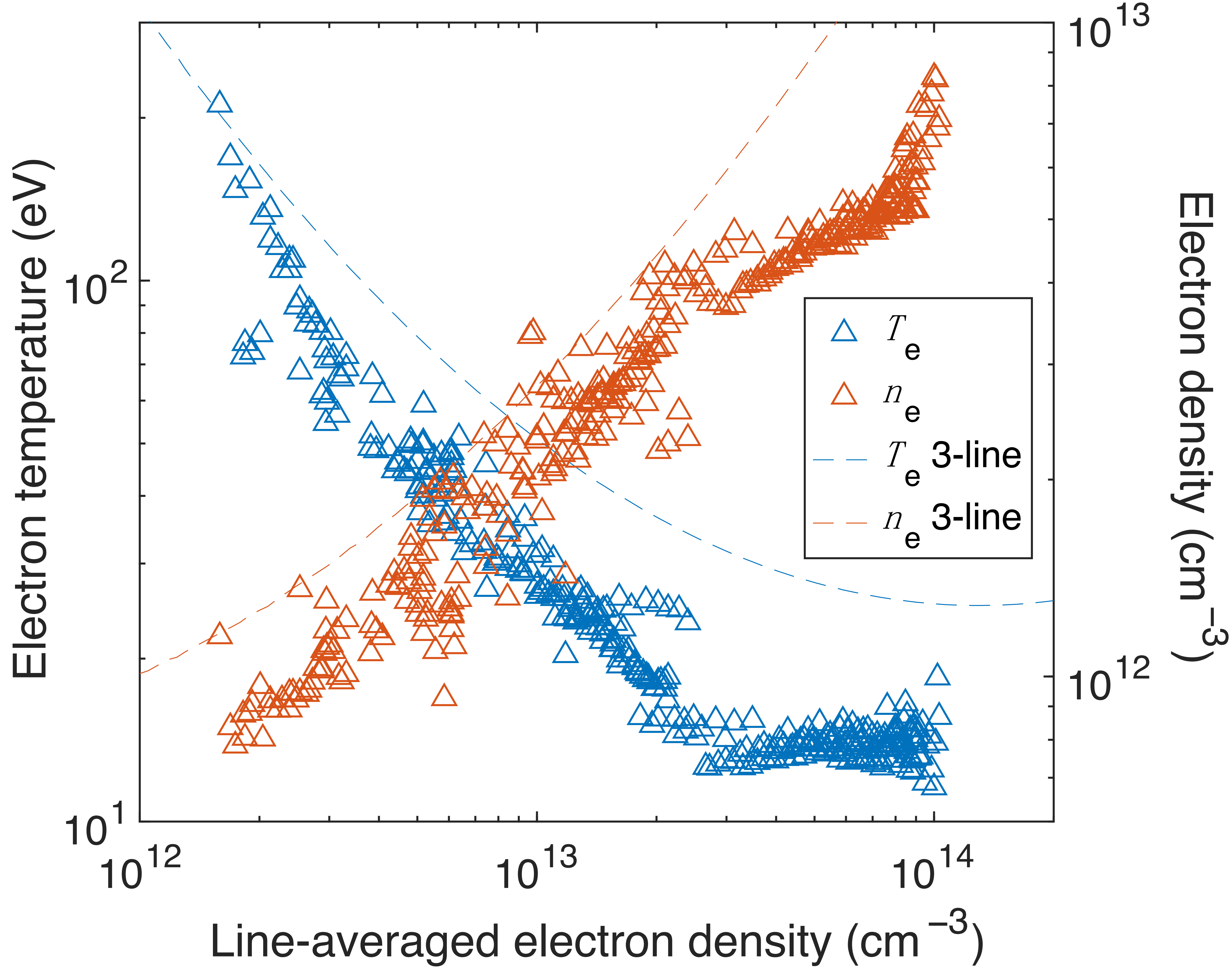

Electron temperature (eV)
Electron density (cm^{-3})
Line-averaged electron density (cm^{-3})
10^{2}
10^{1}
10^{13}
10^{12}
10^{12}
10^{13}
10^{14}
T_e
n_e
T_e 3-line
n_e 3-line

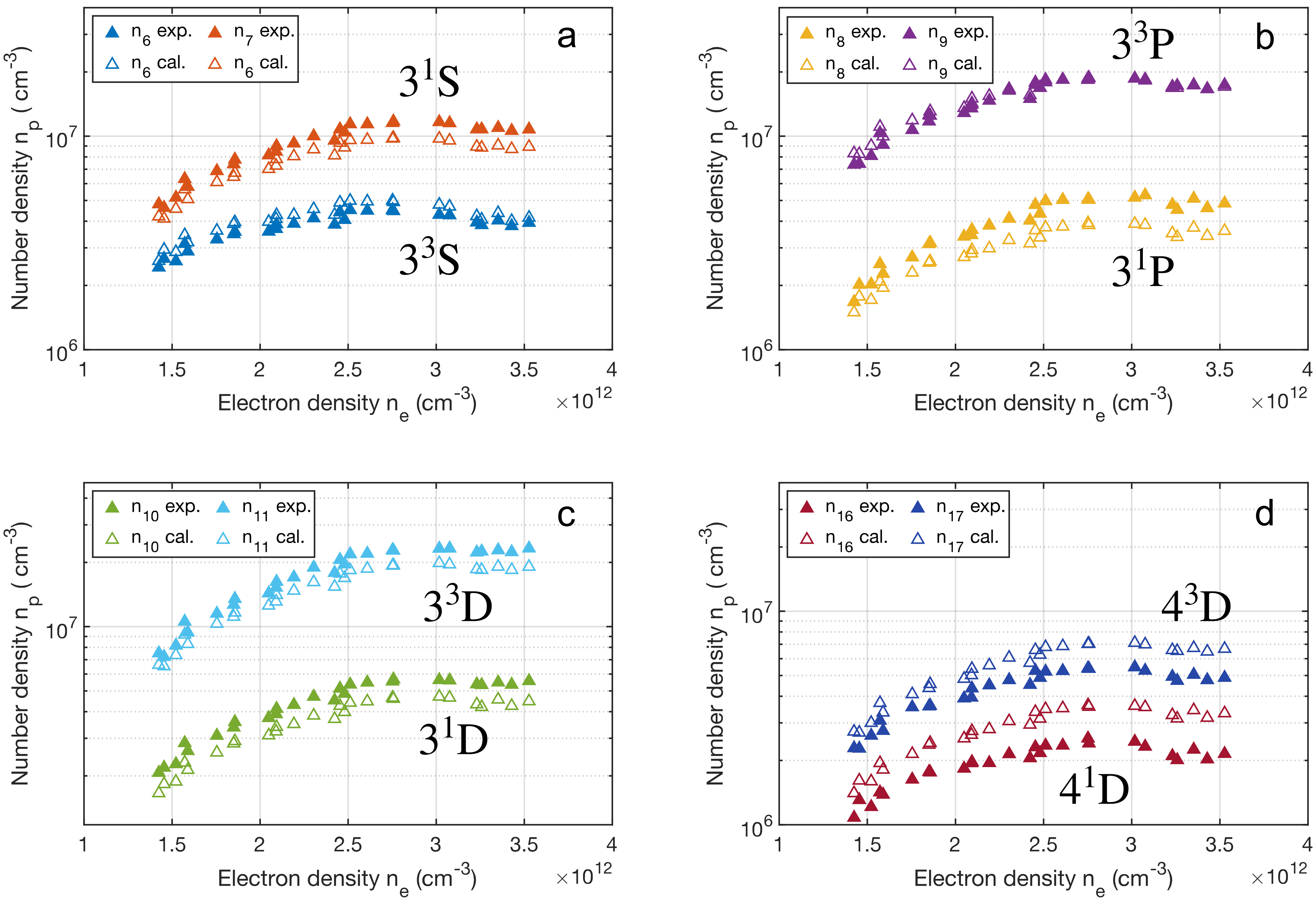
n6 exp.
n7 exp.
n6 cal.
n6 cal.
a
3^1S
3^3S
b
n8 exp.
n9 exp.
n8 cal.
n9 cal.
3^3P
3^1P
c
n10 exp.
n11 exp.
n10 cal.
n11 cal.
3^3D
3^1D
d
n16 exp.
n17 exp.
n16 cal.
n17 cal.
4^3D
4^1D
Number density np (cm-3)
Electron density ne (cm-3)
×10^12
10^6
10^7
1
1.5
2
2.5
3
3.5
4

polarization spectroscopy

- anisotropy in EVDF could play a critical role for the plasma confinement
- polarization spectroscopy is a promising technique for that purpose
- polarization measurement is attempted for Lyman-α line in LHD
- anisotropy in EVDF is evaluated with a help of atomic model

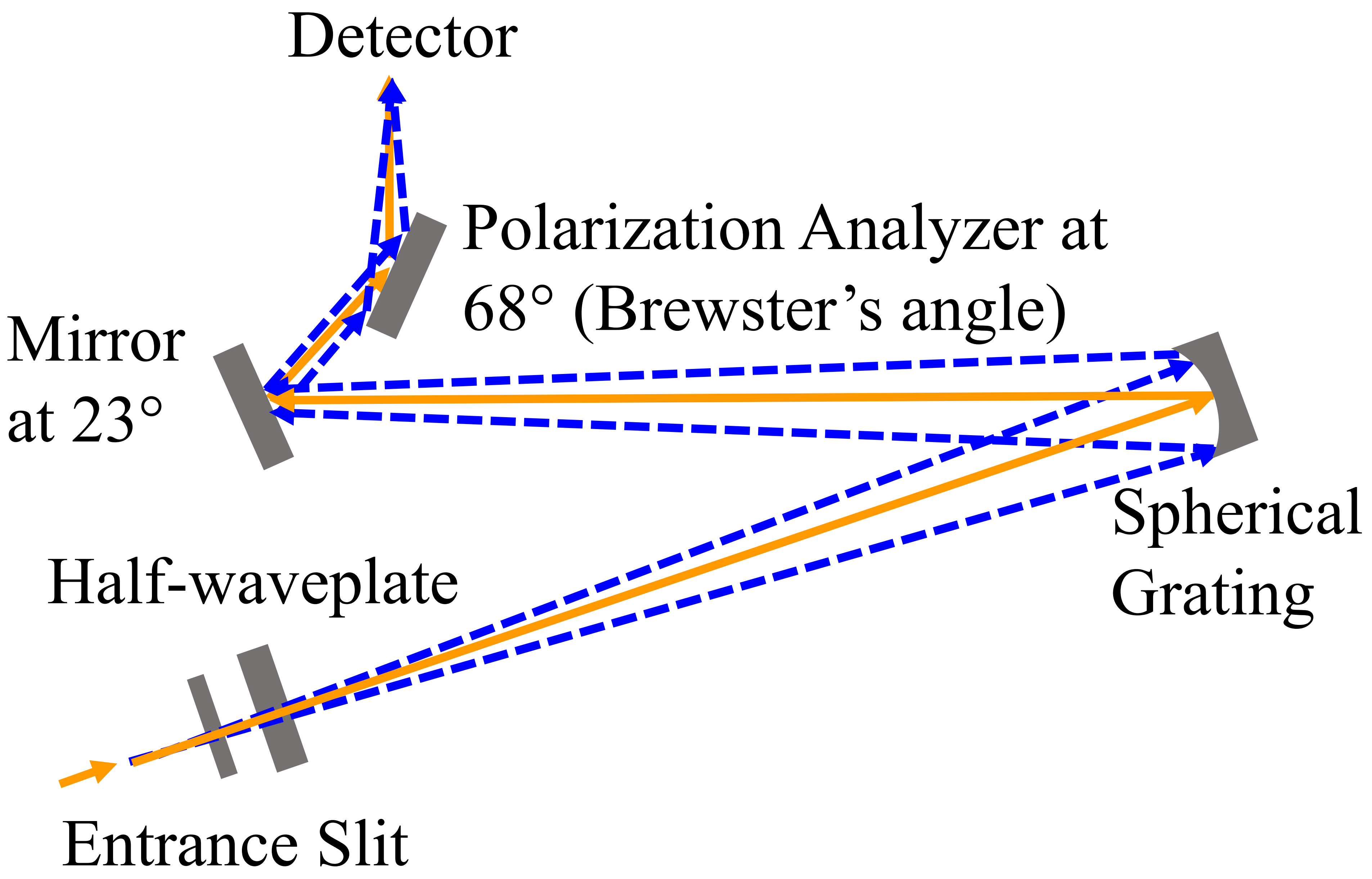

Detector
Polarization Analyzer at
68° (Brewster's angle)
Mirror
at 23°
Spherical
Grating
Half-waveplate
Entrance Slit

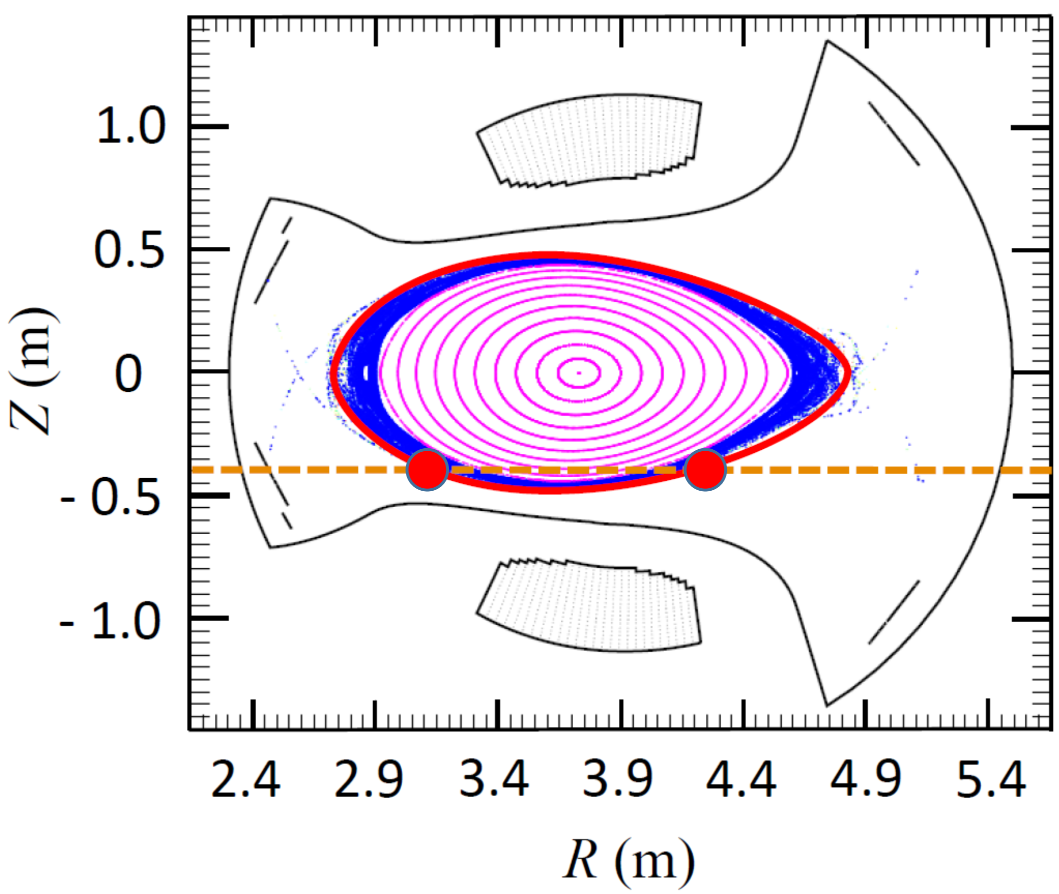
1.0
0.5
0
- 0.5
- 1.0
Z (m)
2.4
2.9
3.4
3.9
4.4
4.9
5.4
R (m)

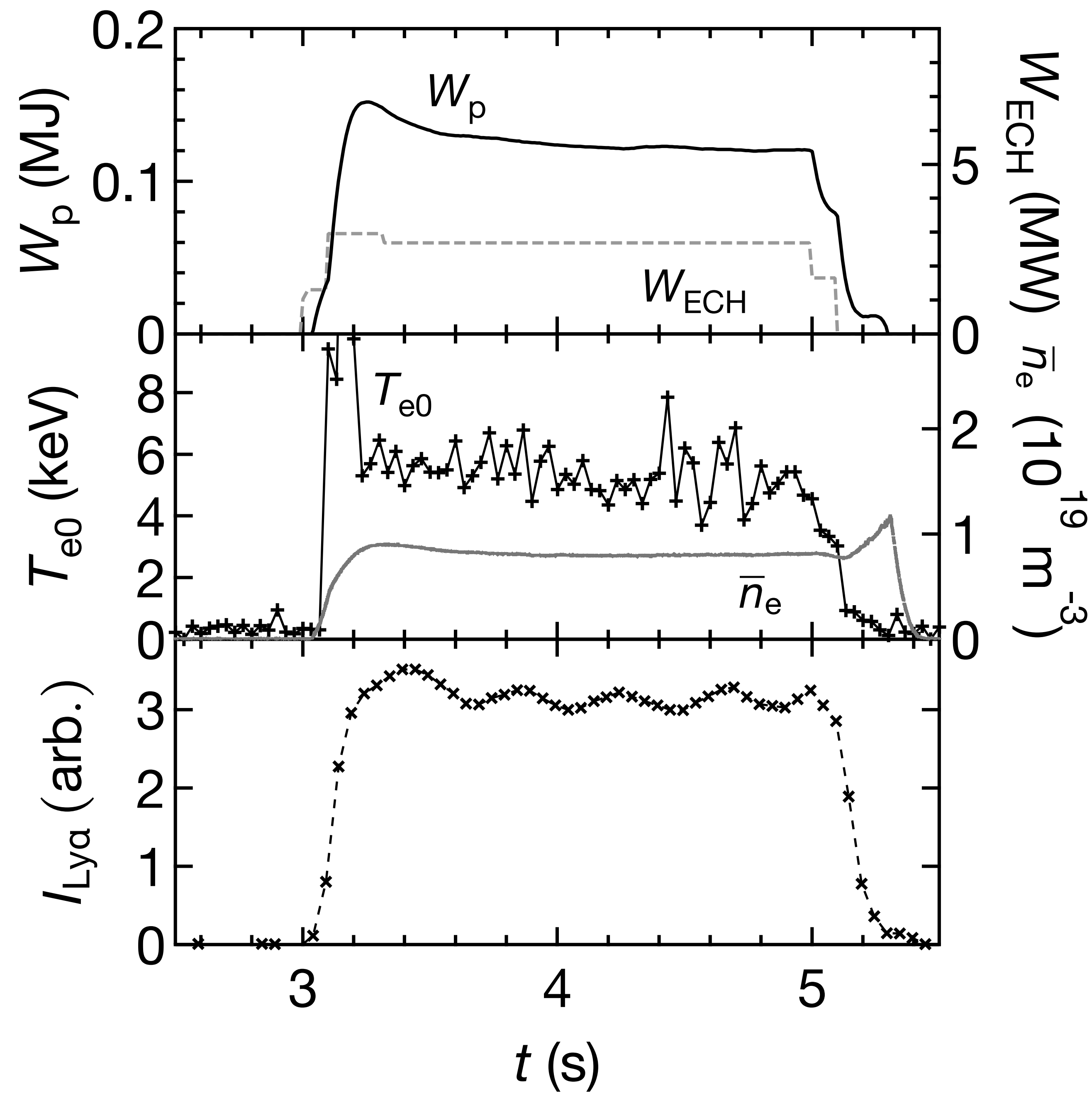
0.2
0.1
0
Wp (MJ)
Wp
WECH
5
0
WECH (MW)
8
6
4
2
0
Te0 (keV)
Te0
ne
2
1
0
ne (10^19 m^-3)
3
2
1
0
ILyα (arb.)
3
4
5
t (s)

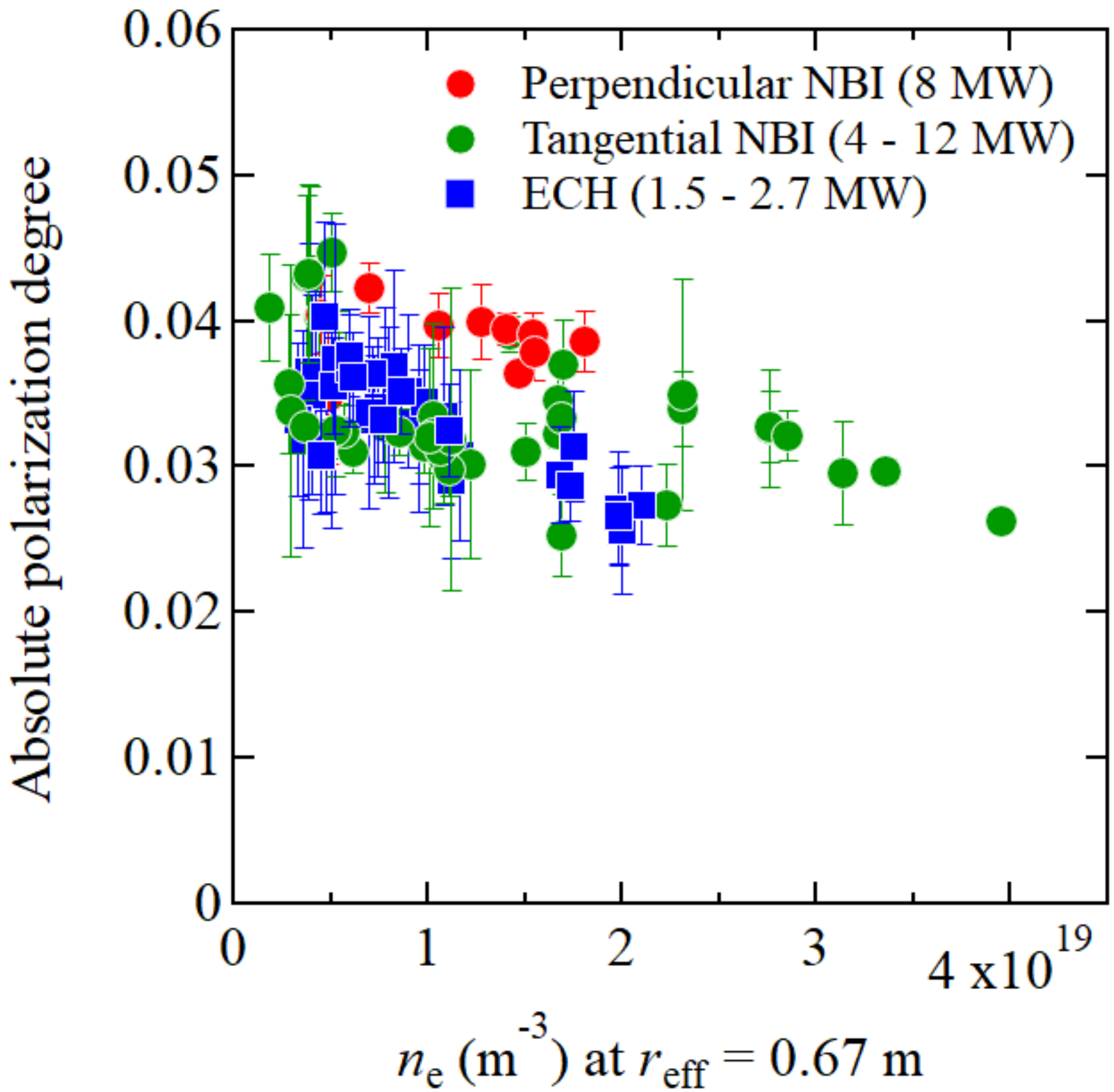

$$P = \frac{I_{max} - I_{min}}{I_{max} + I_{min}}$$

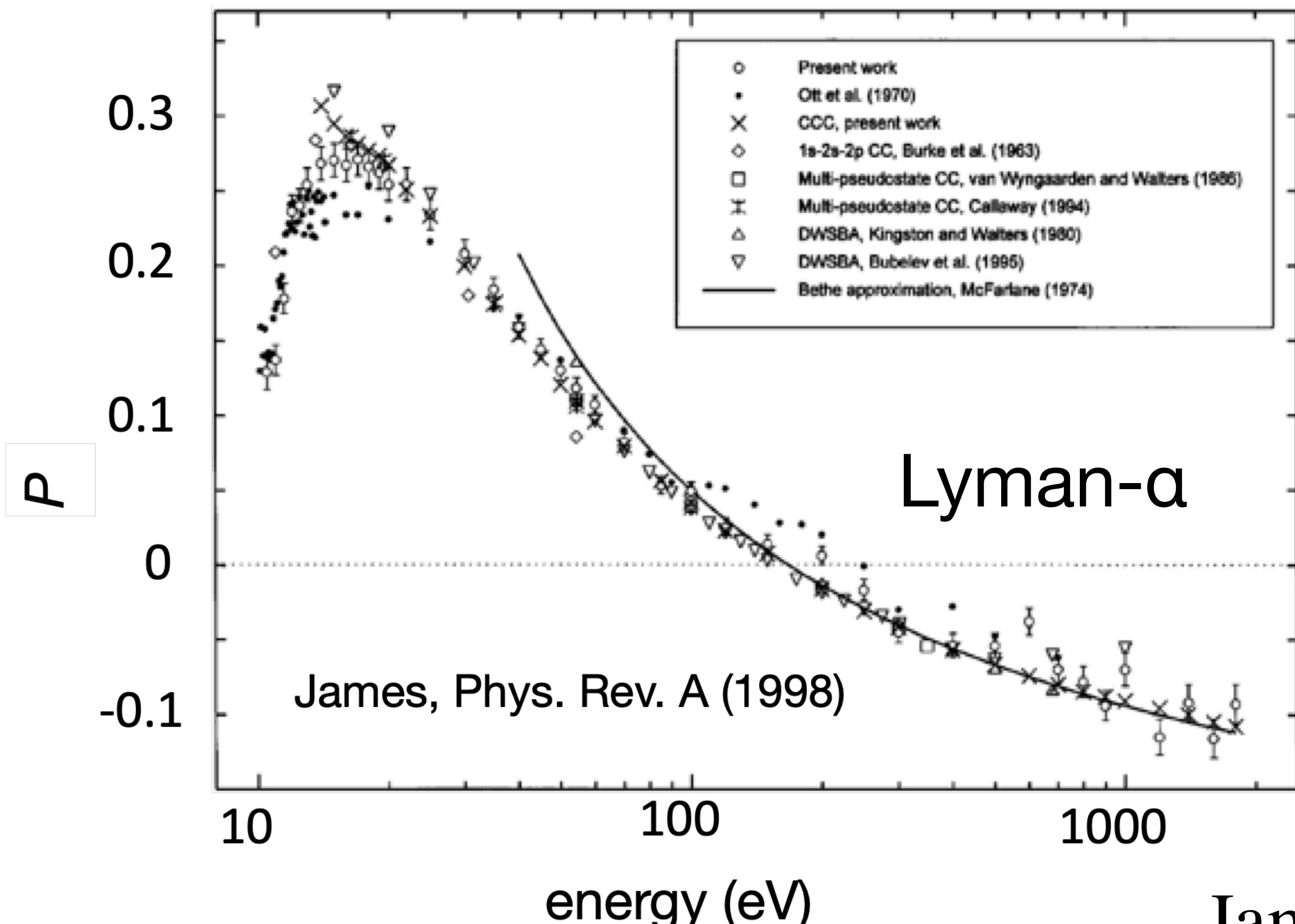

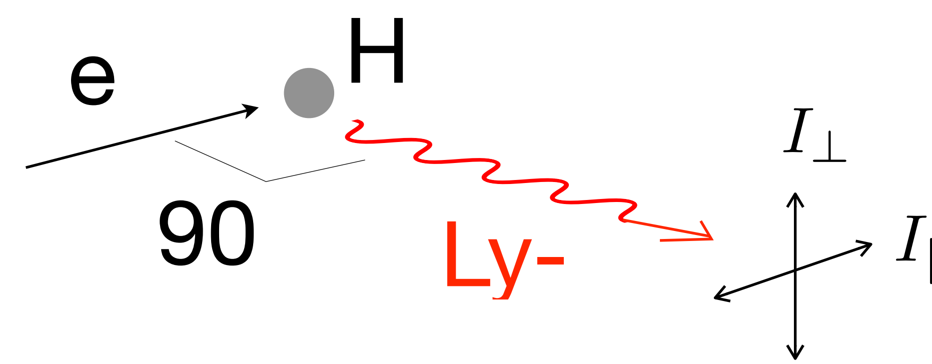

$$P = \frac{I_\parallel - I_\perp}{I_\parallel + I_\perp}$$

James, Phys. Rev. A (1998)

- quantitative analysis of polarization requires a simulation model
- a sophisticated formulation has been developed by Fujimoto (Plasma Polarization Spectroscopy, 2008 Springer)

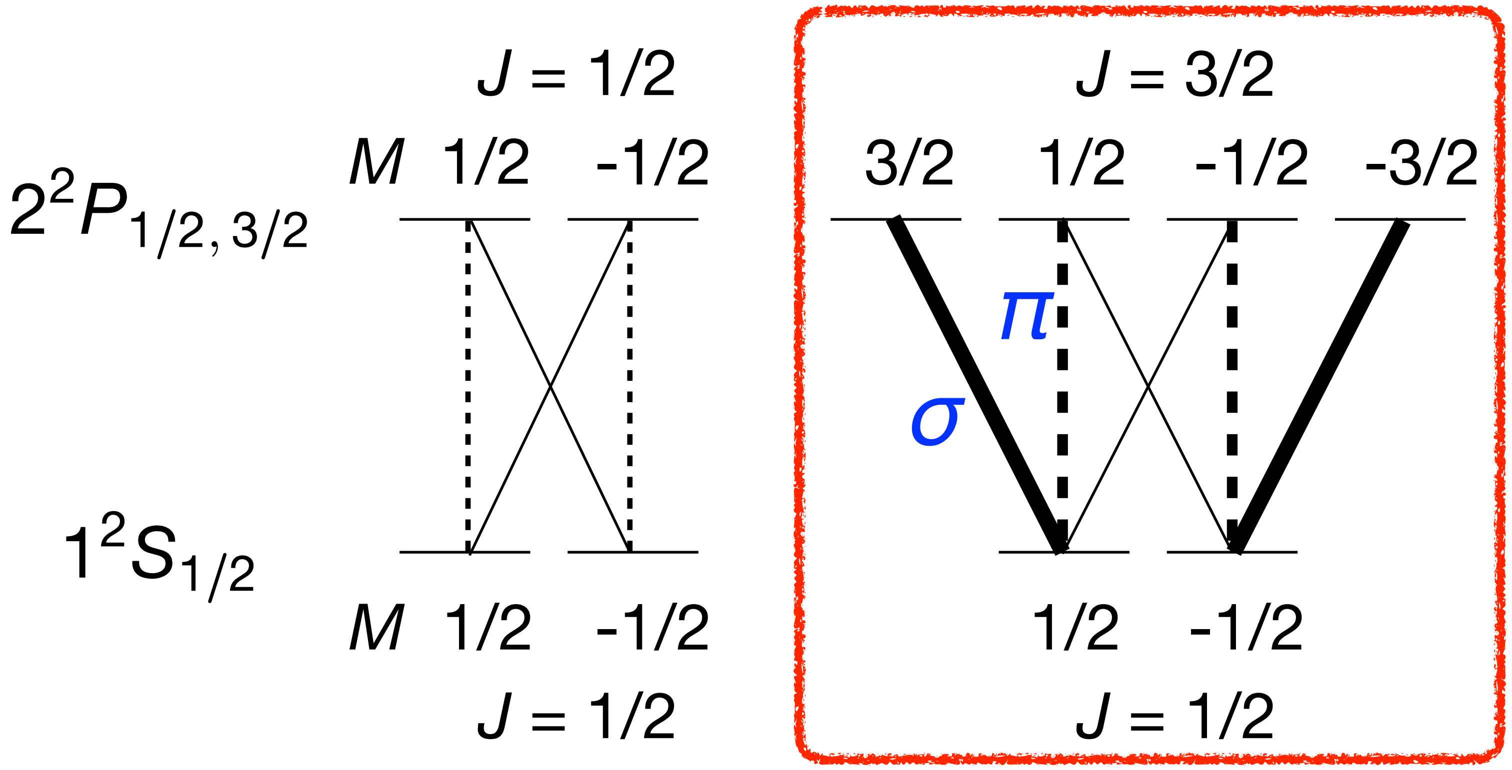

longitudinal alignment

$$A_\mathrm{L} = \frac{I_\pi - I_\sigma}{I_\pi + 2I_\sigma}$$

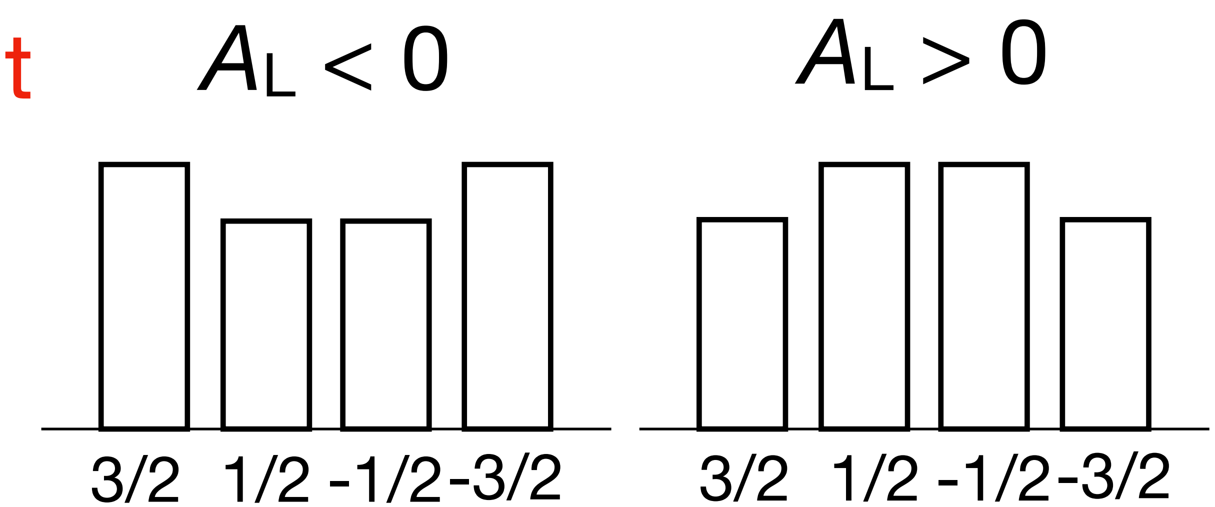

- under axisymmetric condition, density matrix in spherical tensor representation is written by two terms

$$\rho(p) = \underbrace{\rho^0_0(p)}_{\text{population}} T^{(0)}_0(p) + \underbrace{\rho^2_0(p)}_{\text{alignment}} T^{(2)}_0(p)$$

a(*p*) / *n*(*p*) is related to *P* or A_L

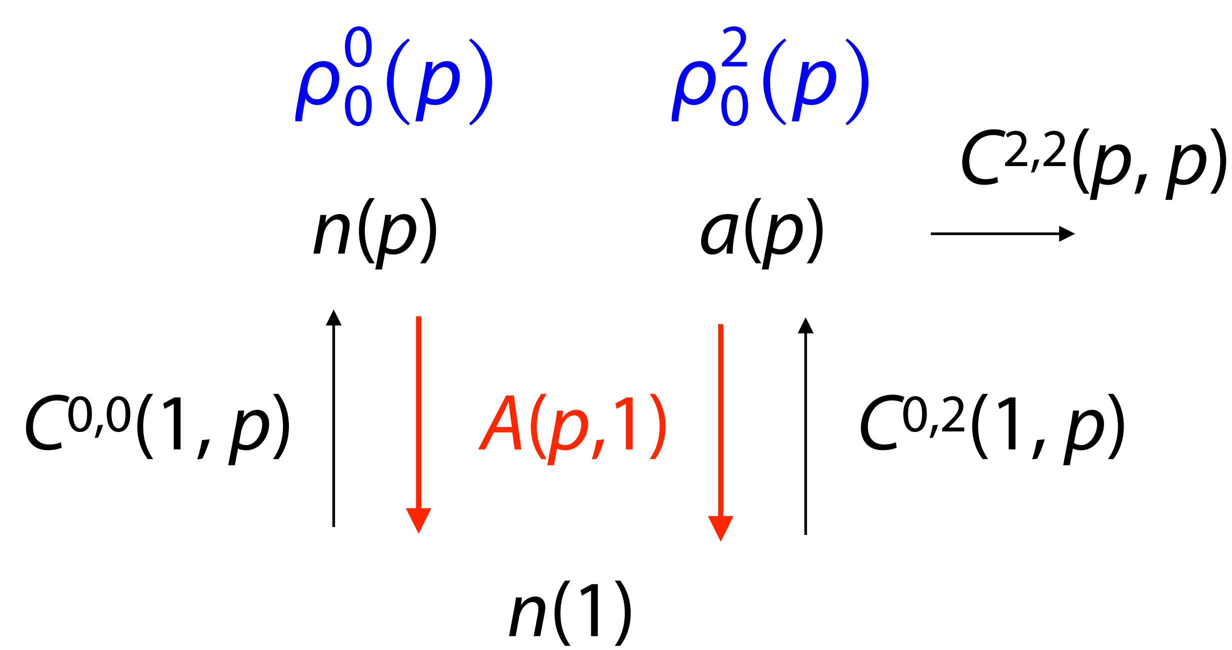

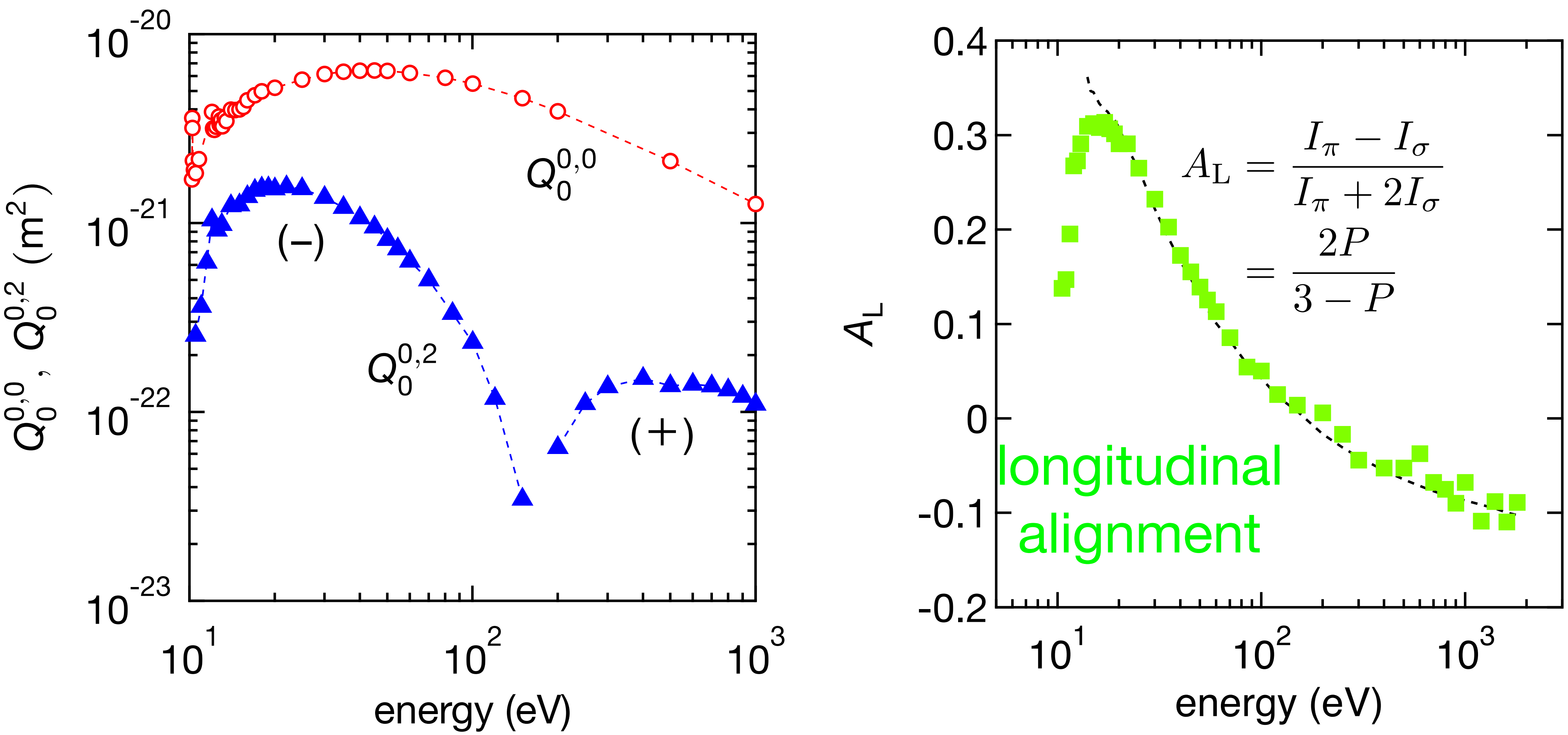

$$Q_0^{0,2}(r,p) = (-1)^{J_p+J_s}\sqrt{\frac{2}{3}}(2J_p+1)^{-1}\left\{\begin{array}{ccc} J_p & J_p & 2 \\ 1 & 1 & J_s \end{array}\right\}^{-1} A_{\mathrm{L}}(p,s)Q_0^{0,0}(r,p)$$

$$f(v,\theta) = 2\pi \left(\frac{m}{2\pi k}\right)^{3/2} \left(\frac{1}{T_\perp^2 T_\parallel}\right)^{1/2} \exp\left[-\frac{mv^2}{2k}\left(\frac{\sin^2\theta}{T_\perp} + \frac{\cos^2\theta}{T_\parallel}\right)\right]$$

$$v_\parallel = v\cos\theta,\ v_\perp = v\sin\theta$$

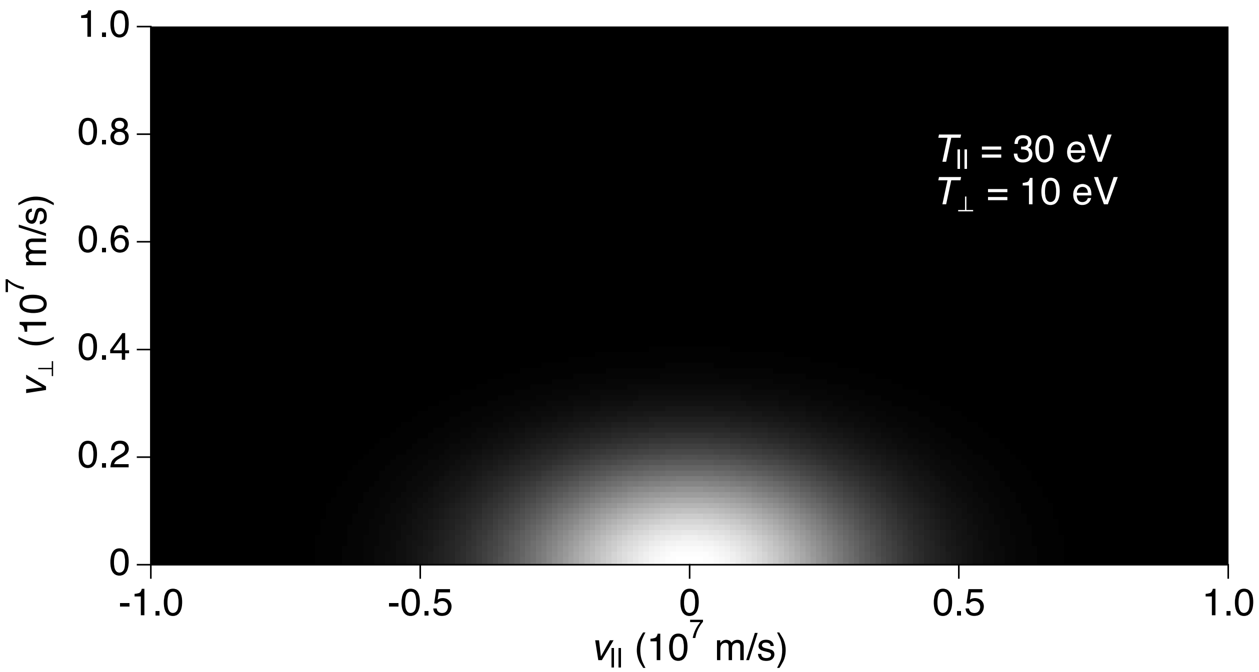

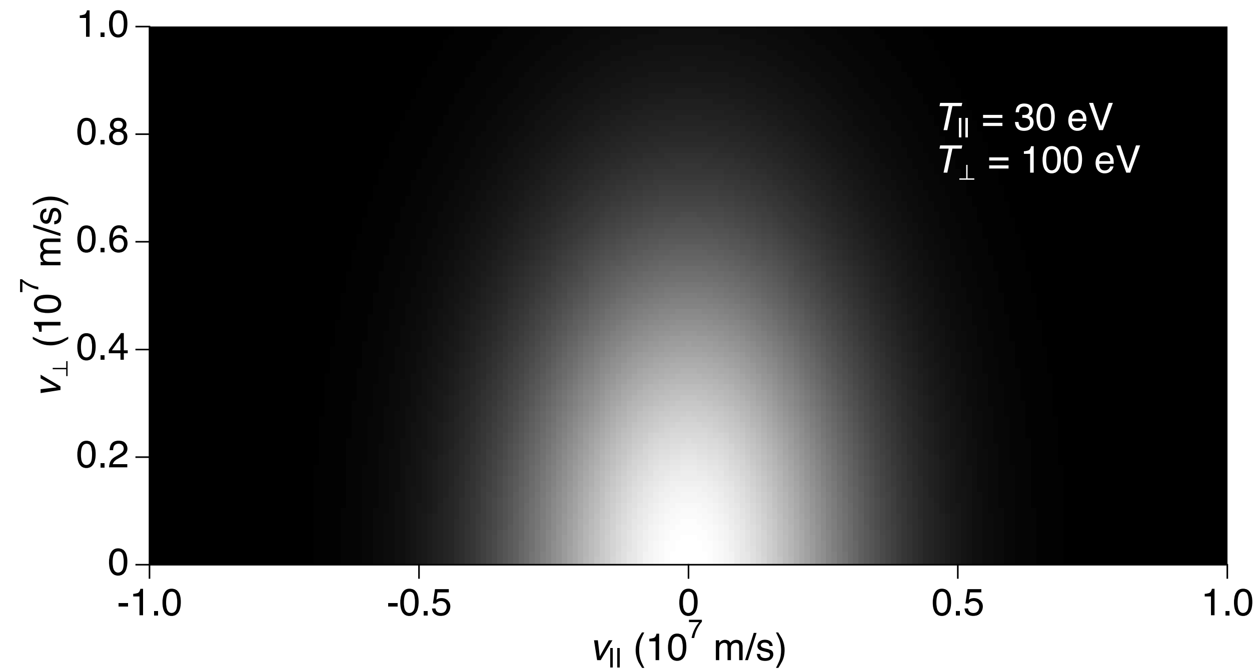

$$C^{0,0}(r,p) = \int Q_0^{0,0}(r,p) 4\pi f_0(v) v^3 \mathrm{d}v$$

$$C^{0,2}(r,p) = \int Q_0^{0,2}(r,p) \left[4\pi f_2(v)/5\right] v^3 \mathrm{d}v$$

$$f(v,\theta) = \sum_K f_K(v) P_K(\cos\theta)$$

$$f_K(v) = \frac{2K+1}{2} \int f(v,\theta) P_K(\cos\theta) \sin\theta \mathrm{d}\theta$$

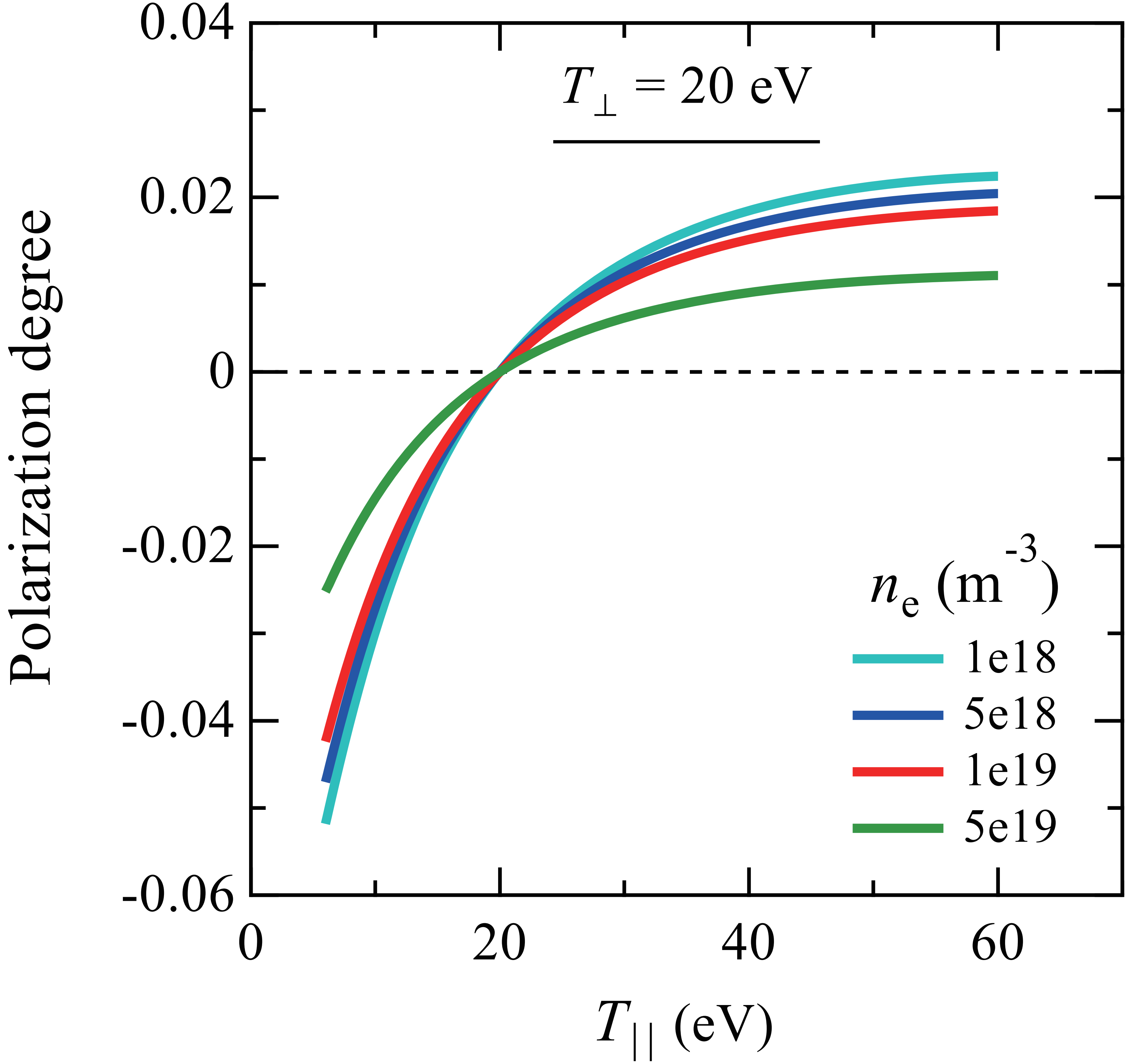

0.04
0.02
0
-0.02
-0.04
-0.06
0
20
40
60
Polarization degree
$T_{||}$ (eV)
$T_\perp$ = 20 eV
n_e (m^{-3})
1e18
5e18
1e19
5e19

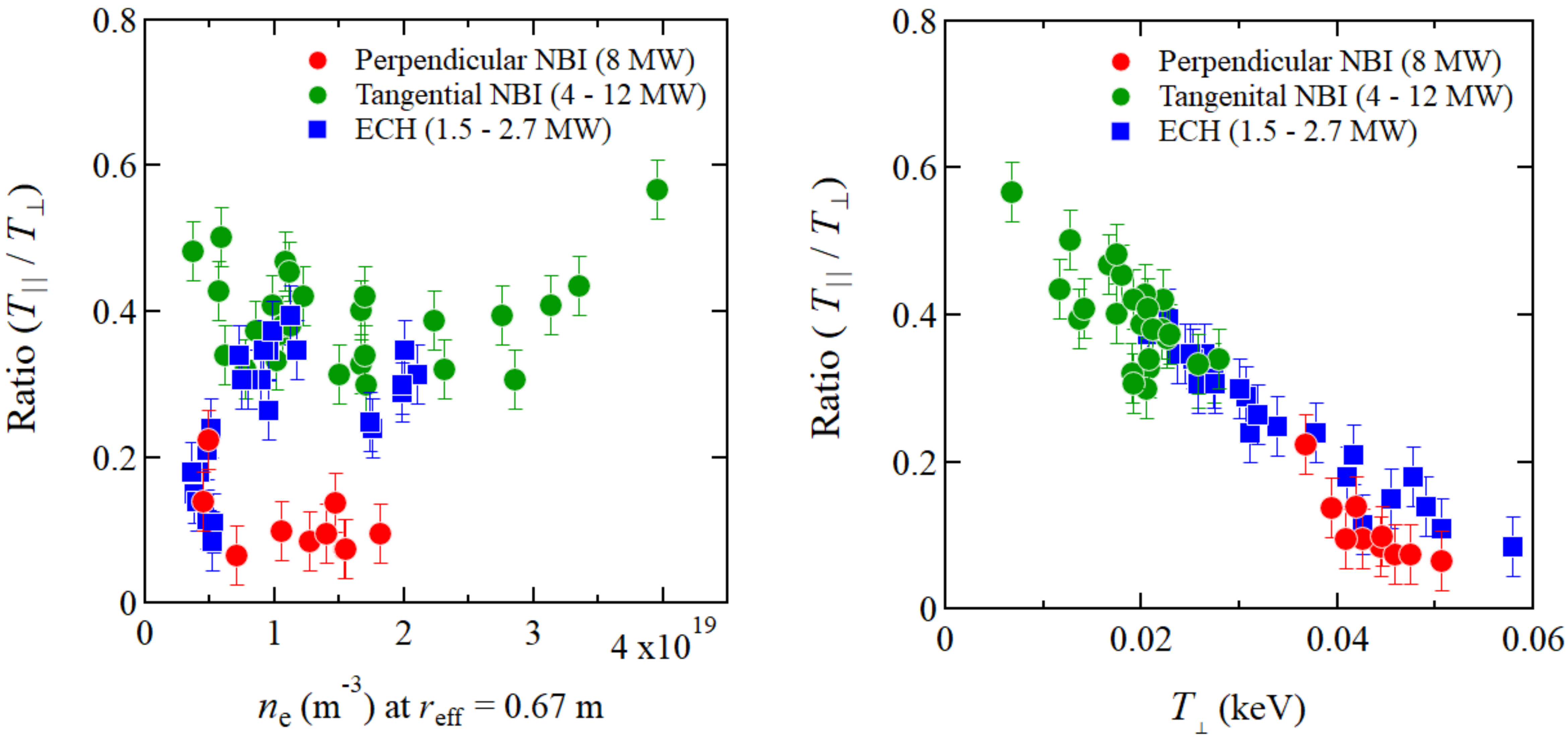

Perpendicular NBI (8 MW)
Tangential NBI (4 - 12 MW)
ECH (1.5 - 2.7 MW)
Ratio ($T_{||}$ / $T_{\perp}$)
n_e (m^{-3}) at r_{eff} = 0.67 m
0
1
2
3
4 x10^19
0.2
0.4
0.6
0.8
Perpendicular NBI (8 MW)
Tangenital NBI (4 - 12 MW)
ECH (1.5 - 2.7 MW)
Ratio ($T_{||}$ / $T_{\perp}$)
$T_{\perp}$ (keV)
0.02
0.04
0.06

- polarization in Lyman-α is detected for plasma of magnetically confined fusion experiment

- anisotropy in EVDF is evaluated in terms of $T_{\parallel} / T_{\perp}$ with the population-alignment collisional-radiative model

- $T_{\parallel} < T_{\perp}$ is always true, that is understandable when particle motion characteristics in the edge plasma are taken into consideration

- anisotropy shows a clear dependence on T_e rather than n_e

ICSLS 2024

26th International Conference on Spectral Line Shapes

2 - 7 Jun. 2024

Prefectural Budokan, Otsu, JAPAN

ICSLS 2024
Otsu, Japan

[Home] [Important Dates] [Program] [Proceedings] [Registration] [Venue] [Committees] [Contact]